



CHALMERS
UNIVERSITY OF TECHNOLOGY

Gas exchange tuning in a single-cylinder research engine model

Replicating multi-cylinder engine gas exchange in a single-cylinder research engine model

Master's thesis in Automotive Engineering

Oskar Edholm
Filip Tagesson

Department of Mechanics and Maritime Sciences
Division of Combustion and Propulsion Systems

CHALMERS UNIVERSITY OF TECHNOLOGY
Gothenburg, Sweden 2021
www.chalmers.se

MASTER'S THESIS IN AUTOMOTIVE ENGINEERING, 2021

Gas exchange tuning in a single-cylinder research engine model

Replicating multi-cylinder engine gas exchange in a single-cylinder research engine model

OSKAR EDHOLM
FILIP TAGESSON

Department of Mechanics and Maritime Sciences
Division of Combustion and Propulsion Systems
CHALMERS UNIVERSITY OF TECHNOLOGY
Gothenburg, Sweden 2021

Gas exchange tuning in a single-cylinder research engine model
Replicating multi-cylinder engine gas exchange in a single-cylinder research engine model

© Oskar Edholm, 2021.

© Filip Tagesson, 2021.

Supervisors: Henrik Salsing, Joop Somhorst
Examiner: Petter Dahlander

Master's Thesis 2021
Department of Mechanics and Maritime Sciences
Division of Combustion and Propulsion
Chalmers University of Technology
SE-412 96 Gothenburg
Telephone +46 31 772 1000

Gothenburg, Sweden 2021

Abstract

The development of new engines is a complex, multi-year endeavor and the process is lined with numerous steps of testing and verification. One of these steps is the use of single-cylinder research engines, which are used to limit variables and enable fast changes of components, methods and strategies when in the early stages of engine development. When the single-cylinder testing is done, the concepts from the single-cylinder are applied in the multi-cylinder engine, this introduces errors, as the pressure dynamics in the intake and exhaust are different in the two engine types due to the number of cylinders and manifold structures. To lessen the impact of this disparity the pressure dynamics in the single-cylinder engine should operate more like the multi-cylinder engine it is trying to replicate.

In this report a GT-Suite model of a single-cylinder engine is created, optimized and verified to closely replicate an existing research engine. The pressure pulses in the intake and exhaust manifold are measured and compared to the ones of a multi-cylinder engine that the single-cylinder is replicating. Thereafter, concepts to modify the pressure pulses are introduced, modelled and tested. The concepts are optimized to modify the pressure pulses in a way that makes them match the multi-cylinder pulses as close as possible. Lastly the effect of altering the cylinder volume of the single-cylinder engine model is assessed.

All proposed designs showed improvement towards replicating the multi-cylinder pressure dynamics and both intake and exhaust utilize the same concept topologically but vastly different in dimensions. This is not unexpected as the pressures on the intake and exhaust behave very differently. This result was verified for multiple engine operating conditions and showed beneficial in all cases.

If the cylinder volume of the engine is altered but all else is kept identical only very minor changes in pressures are observed when compared to the original cylinder volume engine. This is also true when applying the suggested topology modification.

Keywords: Gas exchange, Engine modelling, Optimization, GT-Power, Simulation, Single-cylinder research engine, Multi-cylinder engine.

Acknowledgements

We want to give big thank you to all individuals that have helped in the creation of this thesis, a lot of the work would not have been possible without your dedication. We want to give a special thanks to Henrik Salsing and Joop Somhorst who has supported us as supervisors throughout the project. We also want to thank Zhu Jian, Urban Flock and Magnus Brogeby for your help and support regarding GT-Suite and the various models used throughout this project. Also the people running the research engine, Stina Hemdal and Hannes Wästlund, and for putting up with our questions. We also want to thank Lars-Olof Andersson for the help getting started with the work in a professional setting.

Thank you!

Contents

Nomenclature	xi
List of Figures	xii
List of Tables	xii
1 Introduction	1
1.1 Background	1
1.2 Aim and scope	1
1.3 Research questions	2
1.4 Limitations	2
1.5 Outline	2
2 Theory	3
2.1 The compression ignition engine	3
2.1.1 Engine characteristics	4
2.2 Fuel injection	5
2.3 Combustion	6
2.4 Exhaust gas recirculation diesel engines	7
2.4.1 Internal EGR	7
2.4.2 High pressure EGR	8
2.4.3 Low pressure EGR	9
2.4.4 Cooled and uncooled EGR	9
2.4.5 NOx reduction principles	10
2.5 Valvetrain	11
2.5.1 Main components	11
2.5.2 Valve clearance/lash	12
2.5.3 Timing, lift and duration	12
2.6 Modelling & GT-Power	13
2.6.1 Solver type	13
2.6.2 Discretization	14
2.6.3 Optimization	14
2.6.4 Combustion	14
2.7 Pressure dynamics	16
2.7.1 Multi-cylinder engine pressure dynamics	17

3	Method	19
3.1	Step I: Topology and initialization	19
3.1.1	Mixing tank	20
3.1.2	Optimization	21
3.2	Step II: Joining models, wave tuning and implementing cylinder pressure .	22
3.3	Step III: Topology manipulation and MCE-matching	23
3.4	Step IV: Changing the combustion volume	25
3.5	Model verification	25
4	Results	27
4.1	Step I: Topology and initialization	27
4.2	Step II: Joining models, wave tuning and implementing cylinder pressure .	27
4.3	Step III: Topology manipulation and MCE-matching	31
4.3.1	Intake	31
4.3.2	Exhaust	32
4.4	Step IV: Changing the combustion volume	35
4.5	Model verification over broader range	37
5	Discussion	39
6	Conclusion	41
7	Future work	43
	Bibliography	45
A	Appended figures	47

Nomenclature

Abbreviations

BDC	Bottom dead center
CI	Compression ignition
CN	Cetane number
EGR	Exhaust gas recirculation
EOI	End of injection
EVC	Exhaust valve closing
EVO	Exhaust valve opening
ICE	Internal combustion engine
IVC	Intake valve closing
IVO	Intake valve opening
MCE	Multi-cylinder engine
PM	Particulate matter
RoHR	Rate of heat release
SCE	Single-cylinder engine
SOI	Start of injection
TDC	Top dead center

Physical Constants

μ_v	Volumetric efficiency	—
ρ	Density	$\frac{\text{kg}}{\text{m}^3}$
θ/CAD	Crank angle degrees	°
m	Mass	kg
mep	Mean effective pressure	Pa
N	Rotational speed	RPM
p	Pressure	Pa
r_c	Compression ratio	—
V	Volume	L

List of Figures

2.1	Engine Components.	3
2.2	Schematic engine geometry.	4
2.3	Representative injection profile.	5
2.4	Heat release rate.	6
2.5	High pressure EGR schematic.	8
2.6	Low pressure EGR schematic.	9
2.7	Schematic layout of a basic valvetrain.	11
2.8	Pressure waves in open vs. closed pipes.	16
2.9	Wave dynamics in pipe with changing diameter	16
3.1	System layout.	19
3.2	Schematic of the existing mixing tank.	20
3.3	Representation of the simplified 1D mixing tank.	20
3.4	Recorded pressure at inlet vs. non-optimized simulated.	21
3.5	Possible topology modifications.	23
3.6	Target profile example intake.	24
3.7	Target profile example exhaust.	24
4.1	Recorded pressure at inlet vs. non-optimized simulated.	27
4.2	Inlet manifold pressure comparison. Measured vs. simulated.	28
4.3	Exhaust manifold pressure comparison. Measured vs. simulated.	28
4.4	Measured vs. simulated pressure trace.	29
4.5	Back pressure influence on pressure dynamics.	30
4.6	Back pressure controller response.	30
4.7	EGR controller response.	31
4.8	Intake configuration effect on pressure dynamics.	32
4.9	Exhaust configuration effect on pressure dynamics.	33
4.10	Schematic of the final optimized design.	33
4.11	Notation description.	34
4.12	Volume effect on intake pressure dynamics	35
4.13	Volume effect on exhaust pressure dynamics	35
4.14	Comparison of pressure dynamic responses based on volume in the intake.	36
4.15	Comparison of pressure dynamic responses based on volume in the exhaust.	36
4.16	Comparison of pressure dynamic responses, in the intake. 700rpm 85Nm.	37
4.17	Comparison of pressure dynamic responses, in the intake. 1400rpm 472Nm.	37
4.18	Comparison of pressure dynamic responses, in the exhaust. 700rpm 85Nm.	38
4.19	Comparison of pressure dynamic responses, in the exhaust. 1400rpm 472Nm.	38

List of Tables

2.1	Optimization algorithms	15
2.2	Combustion models	15
3.1	Load cases used for optimization.	21
3.2	Cylinder dimensions.	25
3.3	Verification load points.	25
4.1	Exhaust valve pressures on both sides of valve.	29
4.2	Dimensions of best design concepts.	34

1 | Introduction

This report describes the development of gas exchange GT-power models for two single-cylinder research engines with different cylinder volumes (13L & 16L). Those models are analyzed and compared to a set of multi-cylinder models to see the differences and similarities. Furthermore, possible hardware modifications and additions that can replicate the gas movement and dynamics in a multi-cylinder engine closer are analyzed. With the suggested modifications to the intake and exhaust, the effect of modifying cylinder size is assessed, to see if the gas exchange is still representative of its multi-cylinder version.

1.1 Background

Internal combustion diesel engines are the main engines used by the transport industry today [1]. Due to stricter and stricter emission regulations the development of alternative engine types and fuels is necessary [2, 3]. Thus far, no other engine type can outperform the internal combustion engine (ICE) in long haul applications due to the energy density and availability of the fuel. Battery electric and fuel cell electric counterparts still suffer from slow charge times, low fuel availability, shorter range and higher weight. Therefore it is expected the ICE most likely will remain as a large contributor in the transport industry for years to come, but their continued development is still needed to reduce emissions and improve efficiency [4, 3].

Single-cylinder engines (SCE) play a significant role in the development of all types of ICE's. The single-cylinder research engine gives larger flexibility on the analyses done and is regarded as a less complex system than a multi-cylinder engine (MCE). Today there is a large difference between the gas management systems on single-cylinder research engines and multi-cylinder production engines. Oftentimes, it would be beneficial if the single-cylinder engine was operated in the same way as the multi-cylinder engine it is mimicking. Therefore, in this project, a set of gas exchange models was created and calibrated to make a gas exchange model of a single-cylinder engine behave like a multi-cylinder engine. This model can further be used to understand how single-cylinder engine components could be modified or converted to resemble the working conditions of a multi-cylinder engine. As the flexibility of the system also is important, knowing the effect of changing the cylinder volume can be of interest. This would then show if any big errors or limitations occur if the volume is changed.

1.2 Aim and scope

As there are large differences in the air and gas management system between a multi- and single-cylinder engine, it is in most cases advisable to operate a single-cylinder engine in the same way the multi-cylinder engine it should mimic. Thus, the aim of this project is to create a gas exchange model which can replicate these operating conditions. In addition, the goal is for the model to be used for understanding how the single-cylinder specific components can be modified to resemble the conditions of the multi-cylinder engine as much as possible.

In order to reach the aim, the following subtasks are performed during the project:

- Creating and verifying a GT-Suite model of a 16L SCE.
- Defining differences and similarities in gas exchange between SCE- and MCE models.
- Adapting the gas circuit of the SCE model to replicate gas exchange of 6-cylinder model.
- Assessing the effect of modifying the single-cylinder research engine volume.

1.3 Research questions

The research questions are thus:

- Can the gas circuit in a single-cylinder engine be adapted to portray the gas dynamics within a multi-cylinder engine?
- What is the effect of cylinder volume on the gas exchange characteristics in single-cylinder engines?

1.4 Limitations

The project has the following limitations regarding methods, hardware and measurements:

- The project covers one specific SCE at Volvo Group Trucks Technology. This engine has a specific setup custom made for the test cell. The report only takes this setup into account.
- The sensor setup existing before the beginning of the project is used and no new sensors are installed.
- The test data is acquired at specific predetermined load points and further load points are to be explored.
- The main engine simulations are made in GT-suite and specific subsystem data sets are acquired from other softwares.
- The data used to match SCE pulses to MCE is collected from an existing verified MCE-model and no data is collected from a physical MCE.

1.5 Outline

This thesis outlines the theory relevant for the thesis work and for the reader to have an understanding of the method and the results. The modelling in GT-Suite is done in steps to gradually increase the complexity, and explained where large design decisions have been made and relevant information is provided to the reader. All model specific information is not provided in this report and is only available in the model. To conclude this thesis, a final conclusion regarding the thesis objectives is presented along with recommendations for future work.

2 | Theory

ICE vehicles have been and are still the most common type of vehicle in the transport industry and are expected to remain for a long time [1]. The ICE is a machine that converts chemical energy, stored in a fuel, into mechanical energy that can e.g. drive the wheels of a vehicle. This is done by utilizing the released heat and expansion from burning the fuel in an oxygeous environment. The mixture of fuel and air is ignited inside an enclosed space and the increase in pressure drives a reciprocating piston. The full explanation of this engine type is elaborated in Section 2.1. This type of system has been around since the late 19th century and the continued development of such systems is still important to decrease the emissions and increase their efficiency [5].

2.1 The compression ignition engine

As this thesis focuses on the compression ignition (CI) engine this section outlines the theory for this engine type.

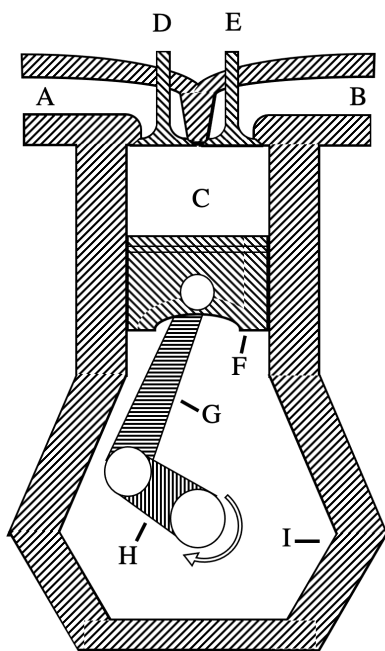


Figure 2.1: Engine Components.

In Figure 2.1 the basic components of a compression ignition engine are shown.

- A - Inlet port
- B - Exhaust port
- C - Cylinder/Combustion chamber
- D - Inlet valve
- E - Exhaust valve
- F - Piston
- G - Connecting rod
- H - Crank shaft
- I - Crank case

First, the piston moves down during the intake stroke the intake valve opens and a new charge of air is induced into the engine through the inlet port. As the piston reaches (about) the bottom most position, bottom dead center (BDC), the inlet valve closes. The piston then moves upwards, compressing the now trapped gas. This compression increases the pressure and temperature significantly. As the piston is nearing the top most position of the cylinder, top dead center (TDC), the injector starts the injection of the fuel, start of injection (SOI). The details of this injection is covered in Section 2.2. The high pressure and temperature within the cylinder eventually causes the injected fuel to self ignite.

This combustion of the fuel increases the pressure and temperature further and forces the piston down with great force. The piston is pushed down during the expansion stroke and the energy is transferred through the connecting rod to the crank shaft where it is transferred on to the transmission and finally the wheels in the case of a car or truck. The piston continues up during which the exhaust valve is open to let the exhaust gases out. After this the cycle repeats. [6, 7]

2.1.1 Engine characteristics

An important characteristic of any ICE is the compression ratio (CR/r_c). This is the volume ratio between TDC and BDC (seen in Figure 2.2) and influences most parts of the combustion properties of any engine. To calculate the CR the volumes at TDC and BDC are required. The volume at TDC is referred to as the clearance volume (V_c). The clearance volume is in a diesel engine often comprised of the volume within the piston, the piston bowl, valve recesses and piston crevices. The piston crown is often completely flat, apart from the piston bowl, and is very close to the cylinder head at TDC. This design localizes the air mainly around where the fuel is injected. The volume difference between TDC and BDC is known as the displacement volume (V_d). Therefore the total volume at BDC is $V_d + V_c$ [6, 7]. From this the CR can be calculated as:

$$r_c = \frac{V_d + V_c}{V_c}$$

Other important engine characteristics and measures can be seen in Figure 2.2 are: the bore (B), the stroke (L), the crank angle degrees (CAD/θ), the crank radius (a) and the connecting rod length (l) [6, 7].

Another important characteristic of ICE's is their volumetric efficiency (η_v). The volumetric efficiency is a measure of how efficient gas is inducted into the cylinder [6, 7]. It is calculated by:

$$\eta_v = \frac{m_a}{\rho_a V_d}$$

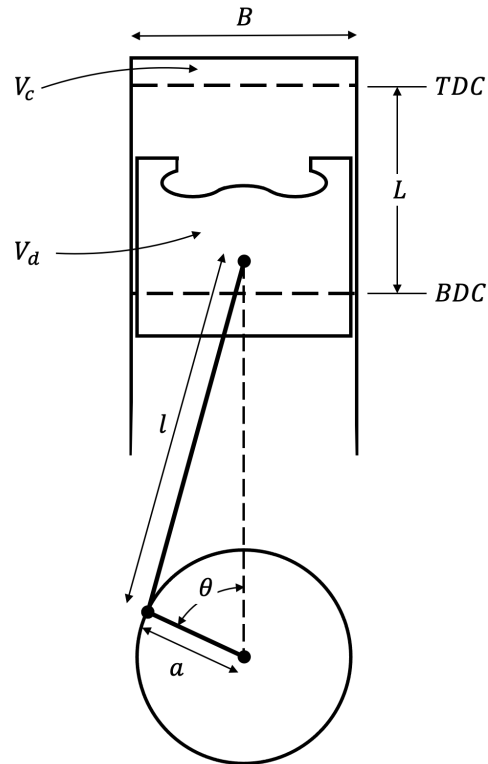


Figure 2.2: Schematic engine geometry.

Where ρ_a denotes the air density at a given reference pressure and temperature. In the case of charged engines the reference pressure is oftentimes the charge pressure but can also be atmospheric. m_a is the total mass of inducted air into the cylinder. When the volumetric efficiency surpasses 1 it is indicative of a system that inducts more air than what would be inducted if a full cylinder were to be inducted at the reference pressure. This can be higher than 1 if pulses are tuned etc. [6, 7].

2.2 Fuel injection

In CI engines the injection of the fuel is very important and is a complex process. The injection strategy is designed by engine manufacturers meticulously to achieve a lot of different goals, such as decreasing NOx emissions. The SOI is described in relation to the CAD before or after TDC. The end of injection (EOI) is when the injection stops.

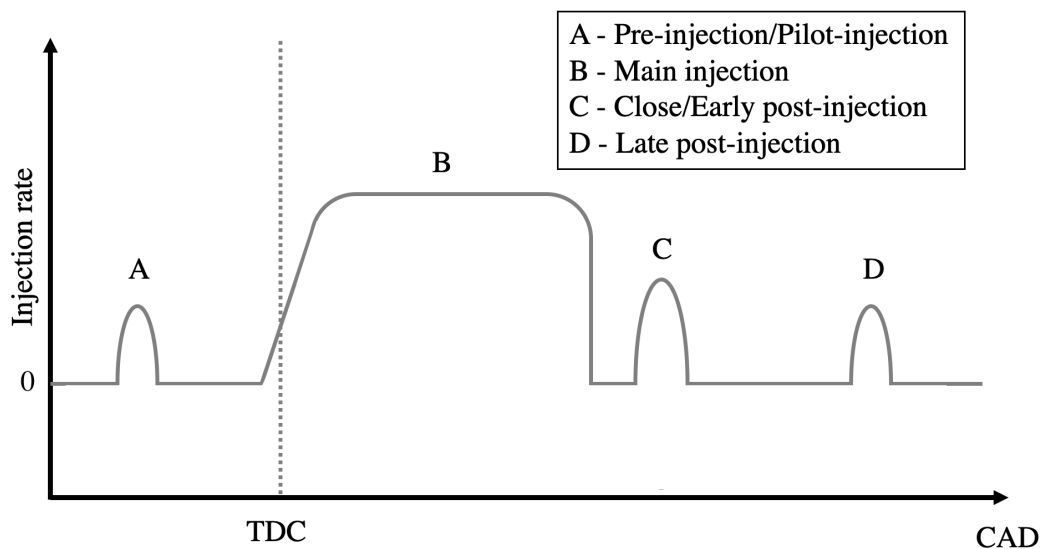


Figure 2.3: Representative injection profile.

The basic components of a multiple injection strategy can be seen in Figure 2.3. As the injection strategy is complex it is often changed according to engine speed and load to give different effects depending on the working condition. The pre-injection(s) is included at lower cylinder pressures to decrease the noise and NOx emissions [8, 9]. The main injection can be formed in many ways depending on the strategy at hand and is the injection that provides the majority of the fuel [10]. The injection rate can be varied during the main injection for injection rate shaping, although it is not very common. This can also reduce NOx emissions. The close post-injection is made to decrease soot formation by oxidizing the soot, and the late post-injection is included when regeneration of the particle filter is needed [8, 9].

2.3 Combustion

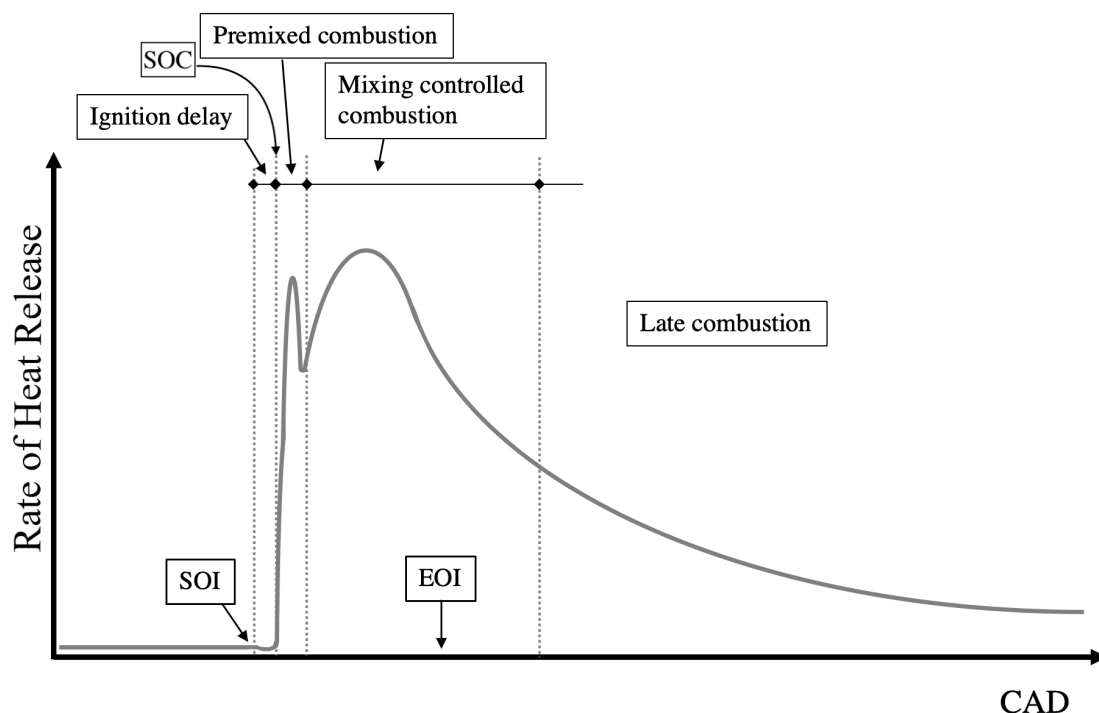


Figure 2.4: Heat release rate.

The rate of heat release (RoHR) depends on several factors in a diesel engine. In Figure 2.4 a generalized representation of the RoHR can be seen with important phases and timings. The injection of the fuel starts at SOI, this is not where the fuel ignites. Initially the release of heat will appear negative as the evaporation of the fuel will draw energy from the system. When the RoHR returns to zero the combustion is regarded as started, the start of combustion (SOC). The time between SOI and SOC is the ignition delay. The extent of the ignition delay is determined by several factors, the pressure and temperature in the cylinder, the injection timing, the oxygen concentration, the Cetane Number (CN) of the fuel, the mechanics of the fuel spray penetration and its atomization, as well as the turbulence in the combustion chamber [6, 7, 11]. During this ignition delay, as the fuel is injected into the cylinder without combustion, the fuel spray will start mixing with the air in the cylinder and reach different levels of air/fuel ratio [11].

The initial combustion step after the ignition is the rapid combustion of the premixed fuel. In this part of the combustion the fuel that has mixed with sufficient air during the ignition delay reach to within the flammability limits is ignited at many nuclei flame sites and spread rapidly throughout the charge. This only requires a few crank angle degrees and the RoHR is quite aggressive as seen in Figure 2.4. This period of the combustion is influenced by the compression ratio, the temperature, the pressure, the mixing intensity and the ignition delay period, while mainly being governed by chemical kinetics [6, 7].

After the premixed fuel has been consumed by the rapid combustion, the mixing controlled combustion phase takes over. This phase of the combustion is mainly controlled by the air/fuel mixing rate while also being influenced by atomization, vaporization and more, most of which are physical limitations.

The combustion can manifest itself with three different end results. The first type is the stoichiometric combustion. This combustion results mainly in carbon dioxide and water. The second type of combustion is rich, which occurs when there is more fuel than available air in the local area. A rich combustion will not burn completely and there will be formation soot and other species of incomplete combustion. The third option is lean burn, which will not burn effectively and produces unburned gaseous hydrocarbons. Each of the rich and lean combustion types can during the combustion mix with either lean or rich areas respectively, and together create a stoichiometric volume where combustion is complete [6, 7, 11].

After the main part of the combustion has taken place there is still some fuel left unburned and some energy still trapped in soot or in energy rich combustion products. Moreover, the burned unreactive products might also isolate fuel and oxygen from each other. These components continues to mix, oxidize and burn at a slower pace as the temperature and pressure in the chamber decreases. During the late combustion, unburned fuel in crevices can also burn, adding to the release of heat [6, 7].

2.4 Exhaust gas recirculation diesel engines

Exhaust Gas Recirculation (EGR) is a system designed to recirculate exhaust gas from the exhaust back to the intake. The purpose of this system is mainly to reduce NO_x emissions. This is done mainly by lowering the oxygen concentration in the cylinder, allowing less oxygen atoms to form NO_x and by heat absorption from combustion products i.e. lower in-cylinder temperature. While the main purpose of the EGR is to lower NO_x emissions there are other purposes, such as improving ignition quality and improving the performance of the exhaust aftertreatment system (EATS). There are several variants of the system, each with its own benefits and drawbacks, presented below [6, 12].

2.4.1 Internal EGR

The first variant is the internal EGR. This is not an added system but is still a form of EGR. Internal EGR refers to the residual gases that go back into or remain in the cylinder during the exhaust stroke. This residual gas is then a part of the mixture for the next combustion cycle. Internal EGR can be done on purpose and be a result of the overall engine design, although it is not always specifically designed. The contributing factors to this are mainly pressure differential, valve timing as well as the pulses in the inlet and exhaust manifold [12].

2.4.2 High pressure EGR

High pressure EGR is a self-driven EGR, meaning the pressure difference between the intake and exhaust pressures are in a ratio making the gases flow from the exhaust side to the intake side. Thus the pressure at the exhaust side needs to be of greater magnitude than at the intake side. On a turbocharged engine this is usually easy, since the EGR outlet can be placed between the exhaust manifold and turbo. This means that the back pressure works in favor of the flow. However, depending on the engine, and especially the turbocharger design, higher intake pressure compared to back pressure can be reached under certain conditions, and is most common during high load conditions. This reversed pressure difference works against the EGR flow but can be solved in different ways, including adding a variable geometry turbocharger, which enables EGR-flow by changing the pressure ratio, adding a venturi at the intake/EGR-conjunction or by adding an intake-throttle [6, 12]. Figure 2.5 shows a schematic of a high pressure EGR system.

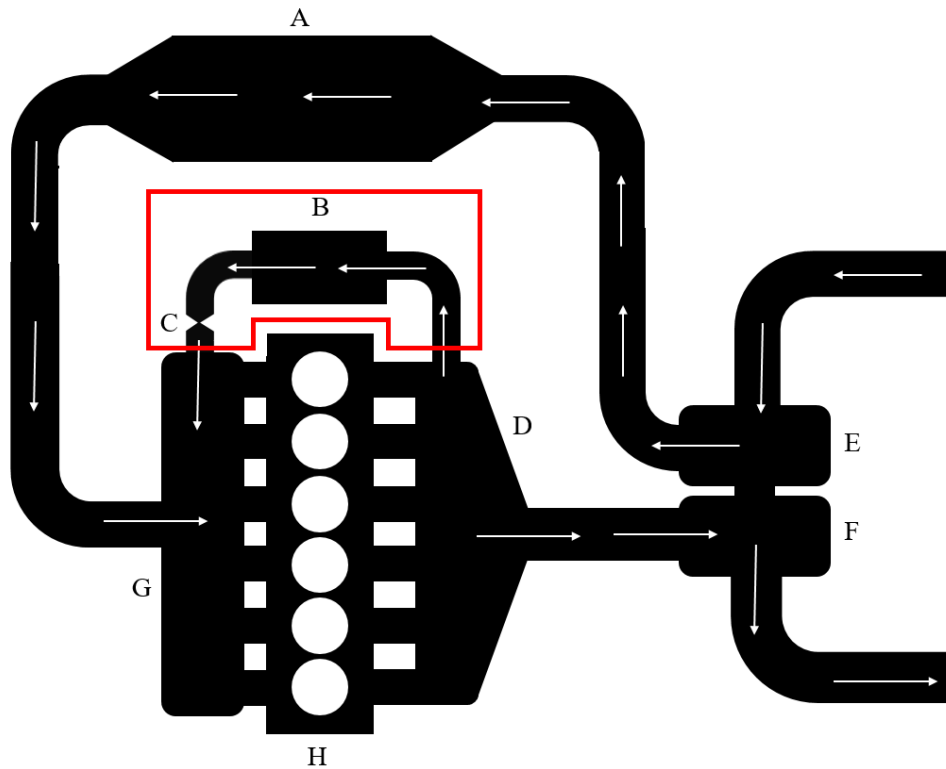


Figure 2.5: High pressure EGR. A: Charge air cooler, B: EGR cooler, C: EGR valve, D: Exhaust manifold, E: Turbo compressor, F: Turbo turbine, G: Intake manifold, H: Engine block.

The high pressure EGR flow is controlled by the EGR-valve located on the EGR circuit. Thus the flow can be controlled depending on load point and overall strategy. One of the drawbacks of the high pressure EGR is that the gases fed through the EGR bypasses the turbocharger and exhaust energy is thus lost.

2.4.3 Low pressure EGR

Contrary to high pressure EGR, low pressure EGR needs assistance transporting exhaust gases to the intake. The system is low pressure due to the placement of the EGR inlet on the exhaust after the turbine. This makes all the exhaust gases available for the turbine on the exhaust side while on the other hand causing the EGR to be re-compressed by the compressor. The EGR inlet can also be placed after the particulate filter giving filtered gases back to the intake. Since the pressure difference cannot be used to transport the exhaust gases to the intake manifold, the gases must instead be fed into the intake before the compressor on the turbo, where the pressure is lower, if no added energy is to be used [12]. Figure 2.6 shows a schematic of a low pressure EGR.

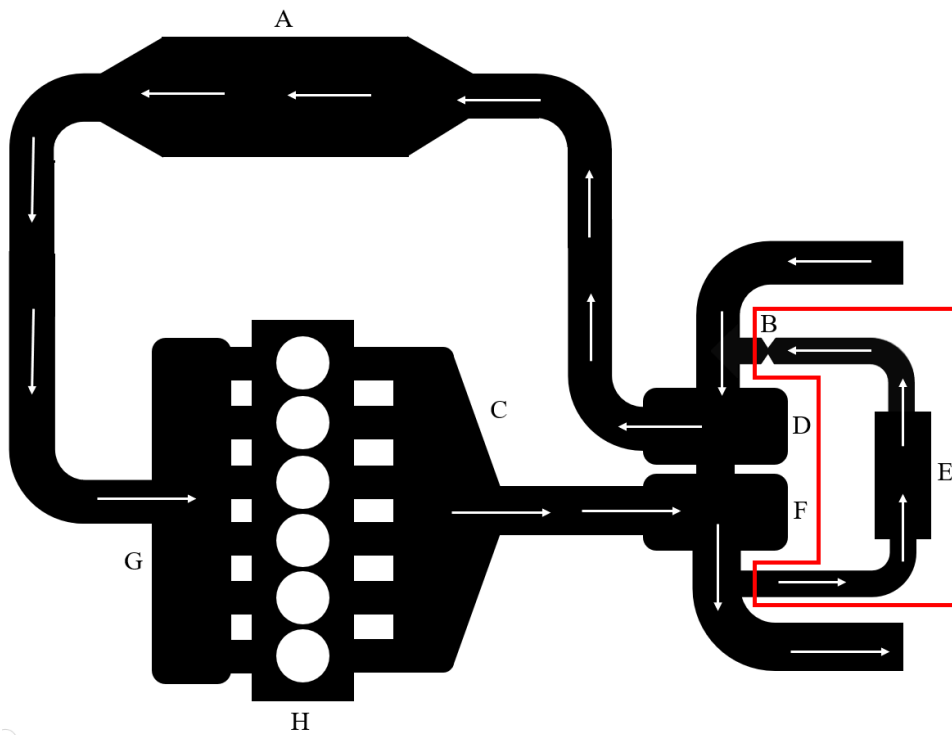


Figure 2.6: Low pressure EGR. A: Charge air cooler, B: EGR valve, C: Exhaust manifold, D: Turbo compressor, E: EGR cooler, F: Turbo turbine, G: Intake manifold, H: Engine block.

2.4.4 Cooled and uncooled EGR

The EGR circuit can either be uncooled (exhaust gases going straight in to the intake) or cooled (exhaust gases pass a cooler before they enter the intake). See Figure 2.5 and 2.6 for cooled systems. If the EGR is uncooled the gases are hotter than the intake air and thus less dense. This setup gives an increase of the average temperature of the charge. The magnitude of the temperature increase does not only depend on the amount of EGR but also on the exhaust temperature and the heat losses occurring in the EGR-system [12].

Uncooled and cooled EGR both have benefits and drawbacks. Uncooled EGR can provide an improvement in combustion stability at lower loads, as well as preventing condensation in the intake manifold and enabling faster engine and EATS warm-up. The drawback of an uncooled EGR is the increase in charge temperature and the affect on the air/fuel ratio, which is of greater magnitude than the cooled system. Therefore, a cooled system can be beneficial at certain operation conditions, as it raises the temperature less. It is especially important at higher loads, the higher air/fuel ratio also provides a higher combustion efficiency and helps lowering the particulate matter (PM) emissions. These two systems can also be combined by having a bypass route around the cooler, resulting in a system that can be cooled or uncooled [12].

2.4.5 NOx reduction principles

There are several ways EGR can lower NOx emissions, the most important one being through lowering the peak temperature of the flame. This can be attributed to four effects, dilution effect, added mass effect, thermal effect and chemical effect. These effects occur simultaneously in real applications and separating them is done to clarify the different effects. According to Ladommatos [13] the four effects can be described as follows:

1. Dilution effect

This effect is reached through oxygen mass reduction, when part of the oxygen in the intake is replaced with inert gas (mainly nitrogen). This is the biggest contributor to NOx reduction of the four. A fixed amount of fuel needs a given amount of oxygen for a complete combustion. When a part of this oxygen is replaced with exhaust gases, the flame needs to broaden to get sufficient oxygen. This leads to a flame zone burning together with an increased amount of non-oxygen molecules that absorbs part of the heat, and this decreases the flame temperature [13].

2. Added mass effect

The added mass effect occurs when the added EGR-gases introduces an increase in the mass flow rate. This added mass flow gives an additional heat capacity to the charge. Not only does the gases have a different heat capacity, which is discussed in thermal effect section below, but the fact that there is a change in the mass flow. This effect is more noticeable for throttled spark ignited (SI) engines than CI diesel engines [13].

3. Thermal effect

The thermal effect is referred to as the change of the average heat capacity of the charge. The change occurs due to the higher heat capacity of especially water and CO₂, which is introduced via the EGR. This is what gives a higher average heat capacity, and it works in conjunction with the dilution effect [13].

4. Chemical Effect

The chemical effect is referred to as energy (heat) consumed by chemical reactions occurring either caused by or with the added EGR-gases. In other words, the added species either actively participate in reactions or dissociate. The reactions consumes energy, meaning energy is taken from the surroundings, and therefore the temperature decreases [13].

2.5 Valvetrain

Controlling the airflow in and out of the cylinders in a four-stroke engine requires a system. That is a task handled by the valvetrain [7]. There exist different solutions of controlling the gas exchange, the most common and the ones used in this project are described below.

2.5.1 Main components

The valvetrain consists of several components, which can be seen in Figure 2.7. The most obvious is the valve itself (B). Its main task is to seal against the valve seat (A) to prevent gases travelling in and out of the cylinders when this is not wanted. There are however other factors that need to be taken into account when designing and implementing a valve. First of all, the angle of the valve in relation to the cylinder axis is important. In a diesel engine the valve angle is usually 0 degrees up to just a few degrees. This is due to the fact that the combustion in a diesel engine occurs in the piston bowl, and that it has high compression ratio relative to a gasoline engine. The volume in the bowl and the clearance volume is optimized for efficient combustion, rather than adding clearance volume to be able to tilt the valves [7].

The valves are required to control the flow, but must at the same time provide enough flow area for the given engine. The flow in to the cylinder through the cylinder head is limited by two main factors. The port and the valve. Initially when the lift starts the flow is determined by the curtain area (the area created between the valve seat (A) and the valve), which in its turn is determined by a function of valve lift. At higher valve lifts the flow is instead determined by the throat diameter of the port [7].

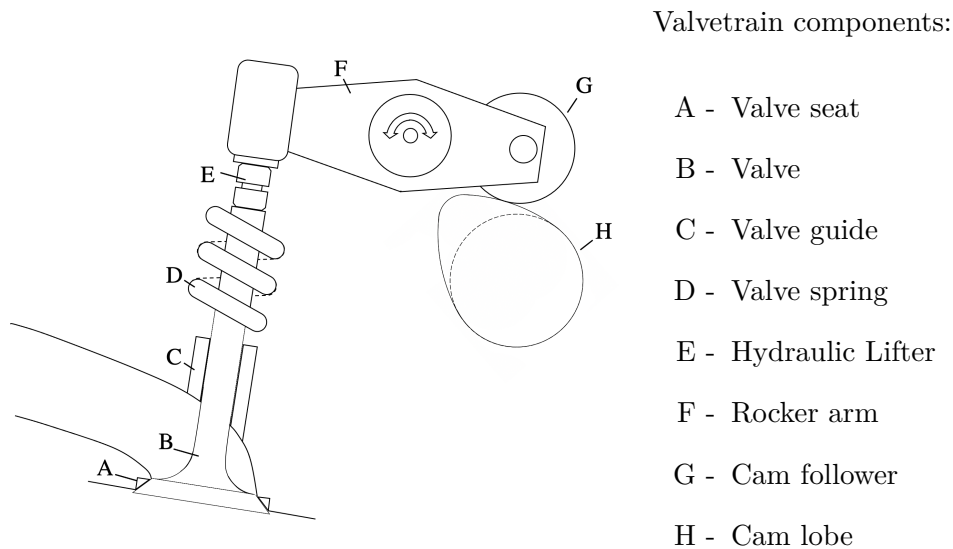


Figure 2.7: Schematic layout of a basic valvetrain.

The flow can be increased by adding more valves, e.g. by instead of having one exhaust- and intake-valve, fitting two of each, or even more. This increases the flow area by enabling better surface utilization. The amount of valves needs to be calculated to ensure maximum surface utilization for the given bore, while other requirements such as the load capacity and thermal resistance are taken into account [7].

To seal, the valve is pressed against the valve seat (A). The valve seat consists of a metal ring pressed into a machined pocket in the cylinder head. This ring is machined after installation to not protrude out of the head and to match the valve angle. The difference in angle between the valve and the seat is small but still relevant, as it makes the contact between the valve and the seat a knife-edge thus sealing well. Up- and down-stream of the valve seat the seat will often be ground to decrease the flow restriction [7]. There can be multiple different angled surfaces on the seat, but only one seals against the valve.

The valves are exposed to high heat which needs to be dissipated somehow, so that the valves do not melt or create hot spots in the combustion chamber. The heat is mainly lead away by heat dissipation through the contact area between the valve and the valve seat and via the valve guide (C). Valves can be filled with different compounds to increase the heat conductivity, such as sodium. Sodium melts at 97.5°C and can thereby increase heat dissipation by increasing the internal heat conductivity. A spring (D) is used o hold the valves pressed against the valve seat when closed. The valve is fitted to this by a valve retainer. This spring also helps the valve keep the contact with the cam or rocker after max lift when the accelerations are the highest. To keep the valve in the right position a valve guide is used. It is beneficial to have low friction between the valve and the guide, why lubrication is required. This is achieved by lubrication with oil, but this oil must be kept from escaping into the ports. This problem is most noticeable during part load when a vacuum can be created in the intake port, mainly in naturally aspirated engines [7].

2.5.2 Valve clearance/lash

The engine runs at different temperatures, from cold starts up to high loads and speeds. This will lead to dimensional changes due to thermal expansion. Different parts of the valvetrain will expand different amounts as different parts will reach different temperatures. To compensate for this, an adequate clearance is built into the system, this is called lash. This clearance is needed between the valve and the rocker arm (F) or the camlobe (H) and the cam follower (G). This ensures that the valve seals against the seat at all temperatures and the valve acceleration is kept within design limits. There are two main solutions to this problem, either keep a physical clearance between the parts, or by using a hydraulic lifter (E). The hydraulic lifter makes sure that it is zero clearance at any time, by utilizing the engine oil pressure, keeping the two parts in contact at all times [7].

2.5.3 Timing, lift and duration

The valvetrain as a whole controls three main functional parameters. The first is the valve timing, this is when the valve is opened. The second is lift, how far the valve is opened and what amount at what time. And the last is the duration, the amount of time the valve is open. In a traditional valvetrain these parameters are built in to the system and cannot change without changing parts of, or the whole valvetrain [7].

2.6 Modelling & GT-Power

GT-Power (GT-Suite) is a software designed and maintained by Gamma Technologies. The software contains several simulation environments that are capable of different analyses, ranging from thermal analysis to combustion and emissions analysis [14]. The software is solving a series of differential equations and provide the user with an easy way of coupling these equations without putting effort into the sub-layer of the software [15]. In this thesis the functionality of the simulation environment GT-Power was used. This environment is designed to simulate and evaluate the engine functionality with a simulated 1D fluid dynamics, heat transfer and flow.

Within the GT-Power software, a model for the engine system analyzed is constructed using blocks and linkages. These blocks represent components in the real engine and its functions. In this thesis the gas exchange is the main modeled property. This includes pipes, heaters, coolers, valves, cylinders, mixing and settling chambers as well as an EGR-circuit [14]. To get the most accurate model, as few major simplifications as possible have been made. As modeling in this type of software always entail some form of simplification minimizing large simplifications is important.

The flow modelling in GT-Suite is based on the Navier-Stokes equations of conservation of momentum, energy and continuity [15]. In GT-Suite these equations are solved in 1D. The whole system is discretized where each pipe and volume is represented by one or several volumes or cells. Within the cells the pressure, temperature, density, internal energy, enthalpy etc. is calculated and assumed homogeneous. The mass flux, velocity, mass fraction fluxes e.g. are calculated at the cell boundary [15]. This is referred to as a staggered grid.

2.6.1 Solver type

The GT-Suite solver can calculate and solve flow in two ways, by either using the explicit or the implicit method [15]. When using the explicit method the solver will calculate new values of mass flow, internal energy and density based on the conservation equations and values from the previous iteration. This gives a general derivative and by using a time step the new value can be calculated. The solver uses values from neighbouring cells to calculate the next step and must therefore have a small time step as to satisfy the Courant criterion (wave dynamics must be captured within each cell for each timestep) [15]. The explicit method is preferred when high frequency pressure wave dynamics are of interest.

The implicit solver is different from the explicit as it solves all sub-volumes of the time step simultaneously by solving the equations iteratively. This method is preferred where high frequency pressure dynamics are not of interest. The method is more CPU demanding per time step but will perform less time steps per cycle.

Due to the nature of the problem at hand the explicit method will be used throughout this project.

2.6.2 Discretization

The discretization of the grid is very important to the results and the convergence of the system. Therefore the sizing of the grid must be taken into account. A too small discretization will result in long simulation run times and unnecessary time spent simulating. On the other hand a too large discretization will result in too fast run time and might not converge properly. The discretization must be evaluated according to pipe lengths and diameters, fluid temperature and more. It is recommended to use $0.4 \times bore$ as the intake discretization and $0.55 \times bore$ as discretization in the exhaust [15].

2.6.3 Optimization

The GT-Suite contains an in-built optimization software that can help the user optimize designs to reach the results the user is searching for [16]. This built-in Integrated Design Optimizer has several different search algorithms suitable for different use cases. The optimizer uses a search algorithm to set new guesses based on the previous results. Some algorithms are preferable when e.g. there are many variables and many local maxima and some when there are few variables and few local maxima. These are presented in Table 2.1. The main optimization target used throughout this project is the “Transient targeting” optimizer, which is set up to give the user the possibility to target a varying signal instead of a constant value [16]. For this the signal must be converted to an objective function, which is done using the following equation:

$$E_i = \sqrt{\frac{\int_{\theta_{start,i}}^{\theta_{end,i}} (X(t)_i - X(t)_{target,i})^2 d\theta}{(\theta_{end,i} - \theta_{start,i})}}$$
$$f = \sum_{signal_i} \frac{w_i E_i}{E_{i,design1}}$$

Where E is the case error, f is the design error, X is the signal and w is the case bias. This gives a clear objective for the function to target and will result in a minimum of 0 when the simulated signal is equal to the measured signal. When using several cases in GT-power the objective functions for each case are added together and the minimum combination wins the optimization. It is also possible to assign different weights to different crank angle ranges. This means the pressure dynamics can be optimized with tougher bias for the induction during intake optimization and for the exhaust stroke during the exhaust optimization [16]. This will result in pressure dynamics that are closer correlated to the measured values during the time the valves are open.

2.6.4 Combustion

In GT-Suite there are several types of combustion models. The definition of combustion progress in GT is the amount of the total fuel transferred from the unburned zone to the burned zone due to enthalpy change [14]. This is used to calculate the RoHR, species and emissions formation. There are more than one combustion model and the ones used in this project are presented in Table 2.2.

Table 2.1: Optimization algorithms available in GT-Power [16]. The algorithm used in the project is based on the case at hand.

Method	Description
DiSCeTe grid	A bisection method that bisects the design space and selects a subinterval to continue to explore. This method should be used where the local variations are low and the design space is continuous.
Simplex	A derivative free Nelder-Mead Simplex method. It should only be used for local optimization.
CMA-ES	Evolutionary algorithm using an open source MOEA Framework. It is recommended for complex single-objective optimization problems.
Genetic, NSGA-III	The genetic algorithm performs a broad search in the entire specified design domain. It is recommended in cases with medium to high complexity with more than three factors. It is also recommended for multi-modal problems and very non-linear problems.
Accelerated Genetic	The same as Genetic algorithm but uses a Kriging metamodel to capture non-linear fits. This model is always recommended over the standard Genetic Algorithm.

Table 2.2: Combustion models [14].

Model	Description
DI Diesel Wiebe Model	This model imposes the burn rate for DICl-engines. It approximates a normal DICl combustion. This is a simple model that uses few inputs but they are hard set and the combustion is not "smart". Therefore it is used for engines where the actual combustion is not the main focus. This model only takes injected fuel mass and air as input.
Three pressure analysis (TPA) Imposed burnrate	This model setup is a backwards calculated imposed burnrate curve. Using collected pressure traces from intake, cylinder and exhaust the model will approximate a suitable burn rate calculated from calculated flows and the recorded pressure. This burnrate can then be reintroduced to the model as a imposed in cylinder pressure.
DI Diesel Multi-Pulse Model	This model is a predictive combustion model that will predict the burn rate and the emissions produced by the combustion in DICl-engines. This model requires calibration from real test data and set the appropriate parameters. This model takes injection, evaporation, mixing and burn into account.

2.7 Pressure dynamics

As the pressure wave dynamics are important in the later stages of this project, a brief overview of the wave dynamics interactions with pipe ends are described. A pipe end can be either open or closed. In the case of a closed pipe end any pressure wave travelling towards the end and bouncing maintains the same sign as the incoming wave had [17]. This can be seen as a spring that is moving along the pipe and when it interacts with the end it is compressed and when the momentum is reversed the spring can decompress and travel back. In the case of an open pipe end the returning wave instead gets the opposite sign compared the original wave. This can be thought of as the wave travelling out of the pipe and “pulling” some of the pressure with it, creating a negative pressure wave that travels back[17]. These phenomena are shown in Figure 2.8.

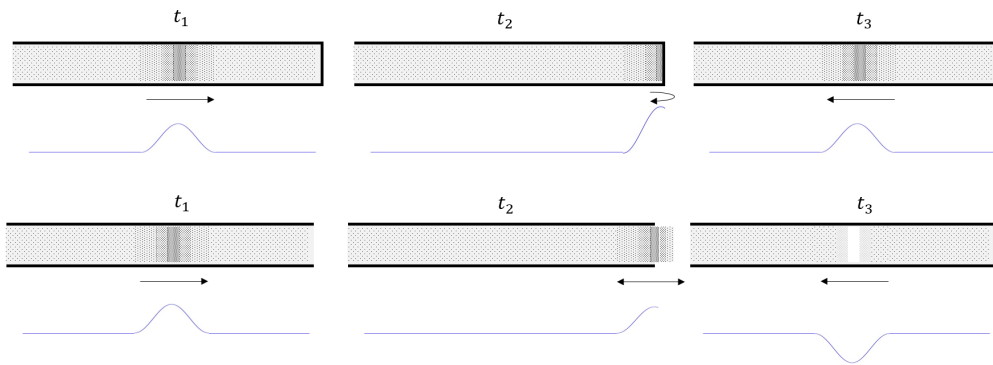


Figure 2.8: Pressure waves in open vs. closed pipes.

When the pipe diameter is changed drastically a similar effect is observed. When the pressure pulses go from a smaller to a larger diameter pipe a similar effect as with the open ended pipe occurs, one pulse travelling back with the opposite sign and one continuing with the same sign [17]. When the pulse travels from a large diameter pipe to a smaller diameter pipe, both pulses will be of the same sign as the original pulse. The effects of these setups can be seen in Figure 2.9.

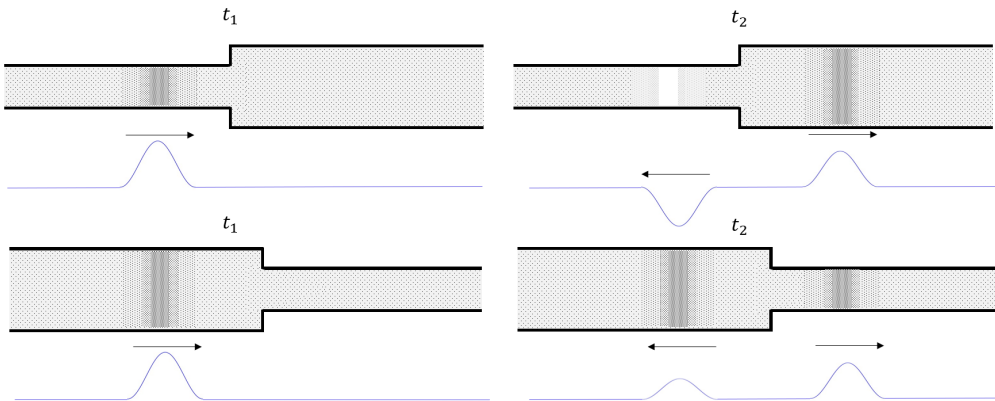


Figure 2.9: The dynamic difference of pressure waves in pipes with increasing diameter vs. pipes with decreasing diameter.

All of these constellations can be combined in a multitude of ways to give a multitude of pressure wave responses and are utilized in Section 3.3 to tune the gas dynamics.

2.7.1 Multi-cylinder engine pressure dynamics

In engines with multiple cylinders connected through a common inlet, pressure pulses originating in one cylinder influences the others. In the intake, the opening of a valve usually results in a negative pressure pulse compared to the average pressure and a positive pulse when the valve is closed. These pulses travels from one cylinder to the others and influence the pressures at the valves, thus influencing the flow and ultimately the amount of charge inducted during the intake stroke. In the exhaust the valve opening results in a positive pressure pulse and oftentimes large fluctuations while the valve is open. The valve closing can result in both a positive and negative pressure depending on the timing. The same effect observed in the intake is present in the exhaust and the valves and pressures influence each other in several ways.

This is sometimes called cross talk and is not present in single-cylinder engines as there is only one cylinder effecting the pressure dynamics in the intake and exhaust. As this can play a large role in the induction and exhaust, this effect is sometimes interesting to replicate as the gas dynamics are important when analyzing engine behaviour.

3 | Method

To create a model in GT-Power with several sensitive controllers and systems, a stepwise approach is often appropriate. This is to ensure that the base systems, such as the main inlet system, is tuned and corrected before EGR circuits and realistic valve events are specified. Therefore the method will consist of a stepwise tuning of the system, in step I the main topology and geometry is considered of the inlet- and exhaust-system and making sure the pressure fluctuations are close to real world cases. In step II the intake and exhaust models are combined, a more accurate combustion model is applied and controllers for backpressure and EGR are implemented. In step III different modifications to the topology are optimized to match the MCE pressure dynamics. In step IV the combustion volume is changed.

3.1 Step I: Topology and initialization

The initial step of creating an appropriate model for the single-cylinder research engine consists of importing the topology of the engine and its relevant adjacent systems. Therefore extensive measurements of the gas circuits need to be conducted. The collected dimensions and geometries are then translated into a corresponding GT-Power model where a cylinder matching the dimensions of the real one is created and a Wiebe combustion model is applied. An overview of this model can be seen in Figure 3.1. The GT model also includes the material properties and surface roughness for correct heat transfer and flow friction. The main focus of this modelling is to achieve a pressure at the inlet and exhaust port as close to reality as possible, as this is where the effect on the combustion is the greatest. The optimization is conducted using measured data collected in the SCE. The effective lengths and diameters are optimized for all relevant parts, to reach pressure dynamics as close as possible to the real world data.

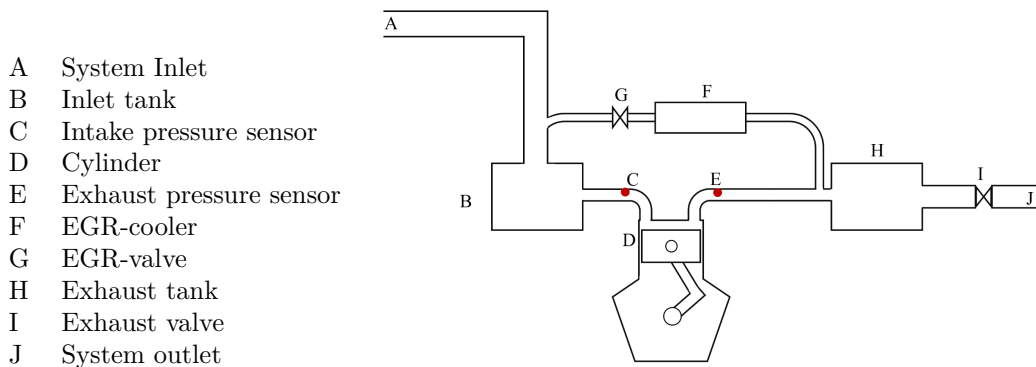


Figure 3.1: System layout.

The boundary conditions for each optimized part are based on an estimated margin of error of the performed measurements. It is not paramount for the dimensions in the model to correspond exactly to the real world, however the model should behave as the SCE. This means that some measurements might be a bit off by design, as they result in the same characteristics as the real world parts.

3.1.1 Mixing tank

On the inlet side of the engine there is a 70 liter tank. The purpose of this tank is to lower the pressure pulses and fluctuations and to mix the EGR, that is entered just before, with the intake air. The topology of this tank is described in Figure 3.2. The thick grey line represents a honeycomb structured insert. This tank is adjacent to the engine inlet and influences the intake pressure characteristics. The tank was modelled in several ways, both in 1D and 3D. The 3D modelling results in a higher accuracy of the flow simulation but at the cost of time. For this reason the system is modelled and optimized in 1D (seen in Figure 3.3).

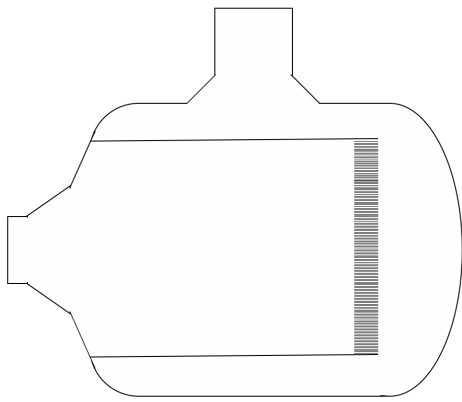


Figure 3.2: Schematic of the existing mixing tank.

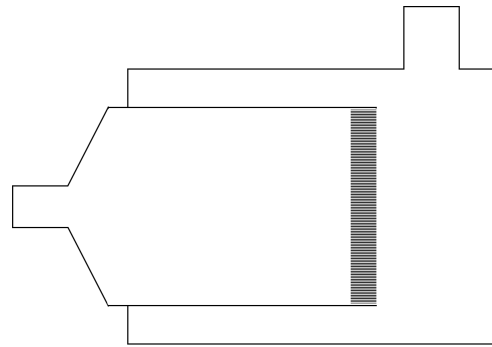


Figure 3.3: Representation of the simplified 1D mixing tank.

Optimizing the inlet side of the engine is done using the built-in optimizer and the target is set as a recorded pressure from the single-cylinder research engine. The tank is simplified for this purpose and some assumptions had to be made, due to computational time. Each part of the simplified model is a 1D part and these are joined together to create a representation of the real tank. The inlet (on top) is modelled as a T junction. The model used can be seen in Figure A.1. The initial real world collected pressure data can be seen in Figure 3.4.

The characteristics of the pressure can easily be seen. The pressure decrease during the intake phase is due to the induction of new charge as the piston moves down. This induction is followed by a slow pressure build up that reaches maximum amplitude at IVO. During the compression and expansion stroke there can be seen small pressure fluctuations in the range of 20-30 CAD between pressure peaks. These peaks can be attributed to internal pressure pulses originating at the inlet valve. During the pressure buildup there are no indications of larger pressure fluctuations, this indicates that larger waves are either suppressed, not created or can travel out of the inlet tank and out of the system.

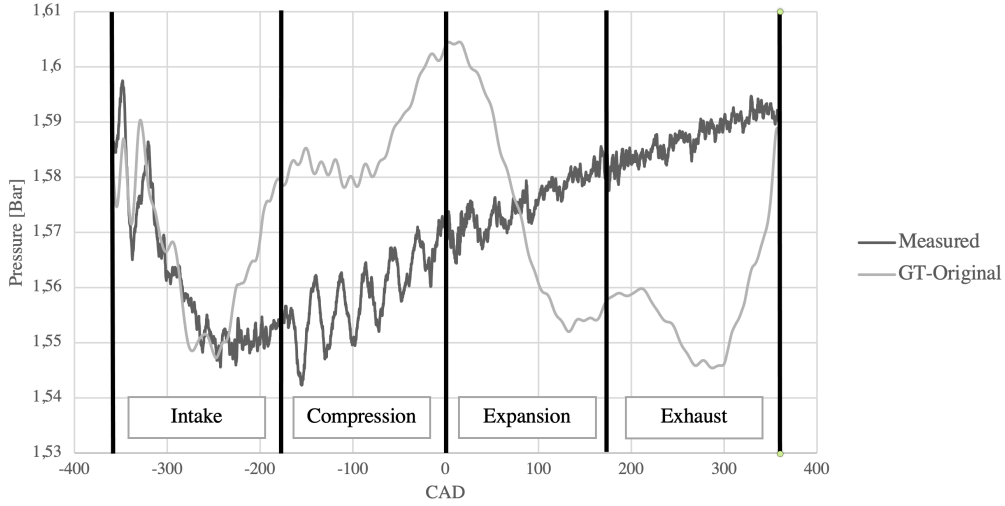


Figure 3.4: Recorded pressure at inlet vs. non-optimized simulated.

In Figure 3.4 the measured and non-optimized simplified GT-power pressure can be seen. This figure shows the obvious mismatch of the pressure dynamics between the two cases. This is due to incorrect dimensions, flow restrictions and temperatures. This is the case for both intake and exhaust which can be seen in Figure A.2.

3.1.2 Optimization

To get the correct pressure dynamics, the system is set up with known fast inlet and exhaust manifold pressure traces from different load cases as a reference. With this known data it is possible to run a large scale optimization that will find specific system dimensions that gives the pressure responses closest to the pressure recorded for the different reference runs. The limits that each individual part is allowed to change its geometry between is based on an assumption of the margin of error for each measurement. This initial optimization is run with different running conditions with regards to speed and torque ranging from 162Nm to 527Nm and 100RPM to 1200RPM. The load points can be seen in Table 3.1. This should give the optimization a speed and torque independent geometry which is important if a universal model is desired. The cases in Table 3.1 are used throughout the project.

Table 3.1: Load cases used for optimization.

Case	Speed	Load	Load*6	EGR%
1	1200	527	3160	0
2	1200	256	1536	15
3	1000	289	1734	8,5
4	1000	162	972	14

3.2 Step II: Joining models, wave tuning and implementing cylinder pressure

In Step I the main topology and the initialization was set. Subsequently, the joining of the two sides is necessary as these have been optimized separately to minimize the amount of variables needing optimization. Also, a more accurate combustion needs implementation as a Wiebe model has been used until now. Therefore, fast pressure recordings at the inlet port, in the cylinder and at the exhaust port are used to tune the combustion to appropriate pressure levels, this is done using the TPA-model described in Section 2.6.4. The measured in cylinder pressure can be seen in Figure 4.4. Using this method also requires the EGR flow to be accurate to the real world engine. Therefore the EGR valve is tuned in conjunction with the back pressure valve as these two will compete if not tuned correctly. The controllers implemented are PID controllers with separate tuning. Therefore it is with this setup possible to evaluate the model using the measured and calculated mass flows in different parts of the engine.

The EGR controller controls the diameter of the EGR valve as a function of the CO₂ in the intake calculated according to the equation below. It is similar to the controller used in the SCE. The function of the optimized controller can be seen in Figure 4.7.

$$EGR_{CO_2} = \frac{Conc.CO_2_{EGR} - 0.04}{15.03}$$

This controller is thus capable of controlling the EGR based on the CO₂ concentration of the charge.

As the exact pressure behind the exhaust valve is unknown, a value had to be selected. The value is set based on the measured value from a sensor behind the exhaust valve that has not been in recent use. The pressure is set to this value but as the uncertainty is presumed high a sensitivity analysis based on this value is carried out.

3.3 Step III: Topology manipulation and MCE-matching

The next step in the process is to initiate the matching of the pressure profiles in the model and the MCE. This matching is carried out using fixed geometry components and non-active elements, such as pipes, flow splits and tanks, to minimize complexity. A series of additions to the flow system are evaluated for expected efficiency in solving the task at hand. These additions are in the form of pipes and splits, the basic topologies are presented in Figure 3.5.

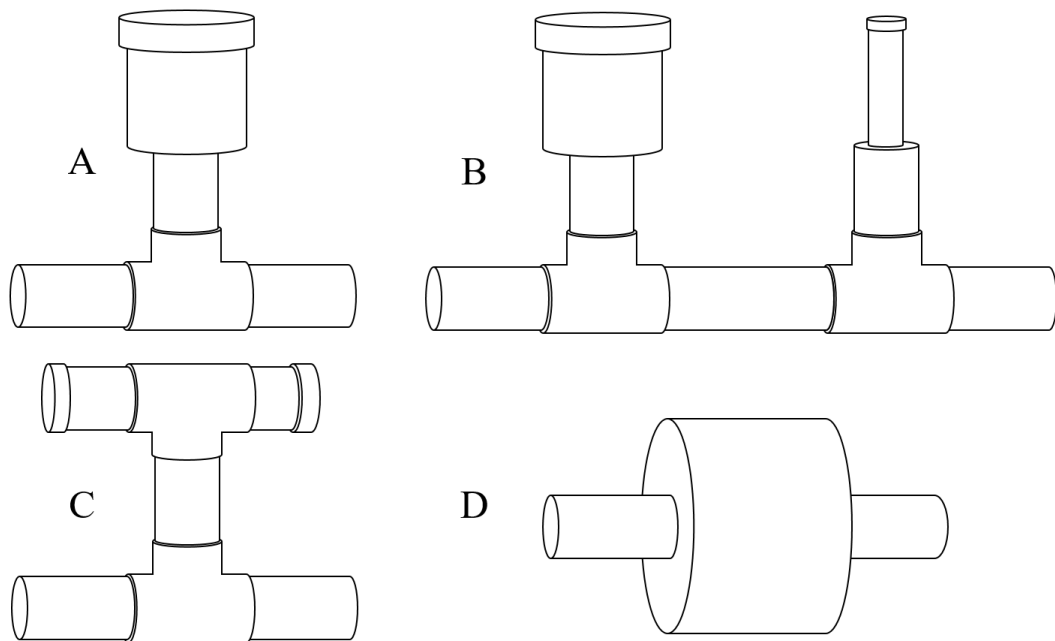


Figure 3.5: Possible topology modifications.

These modifications are added to the intake- and exhaust-side and are allowed to vary in size from very small to very large in all possible configurations within each design. The location of each modification is also allowed to vary but is limited to the general existing geometry of the SCE. On the intake side, the inlet tank will initially be replaced by a pipe of the same size of the inlet and outlet. This is done to reduce the uncertain effects from the tank.

To find the best matching modification and to give them all the best possible chance of success each topology is implemented in GT-power and the dimensions and locations of the modifications are allowed to vary. Note that for modification A and B the outer pipe diameter is allowed to vary from smaller than the inner pipe diameter to much larger. The optimization will thus include the variation on the left of modification B and the right in the same optimization.

To optimize each case a pressure pulse target is set according to Section 2.6.3. The data is collected from verified models corresponding to the MCE that the SCE should imitate. The pressure trace is collected in a similar location as in the SCE and should be representative of the signal that is targeted. One intake trace and one exhaust trace is collected for each case and examples of these can be seen in Figure 3.6 and respectively 3.7.

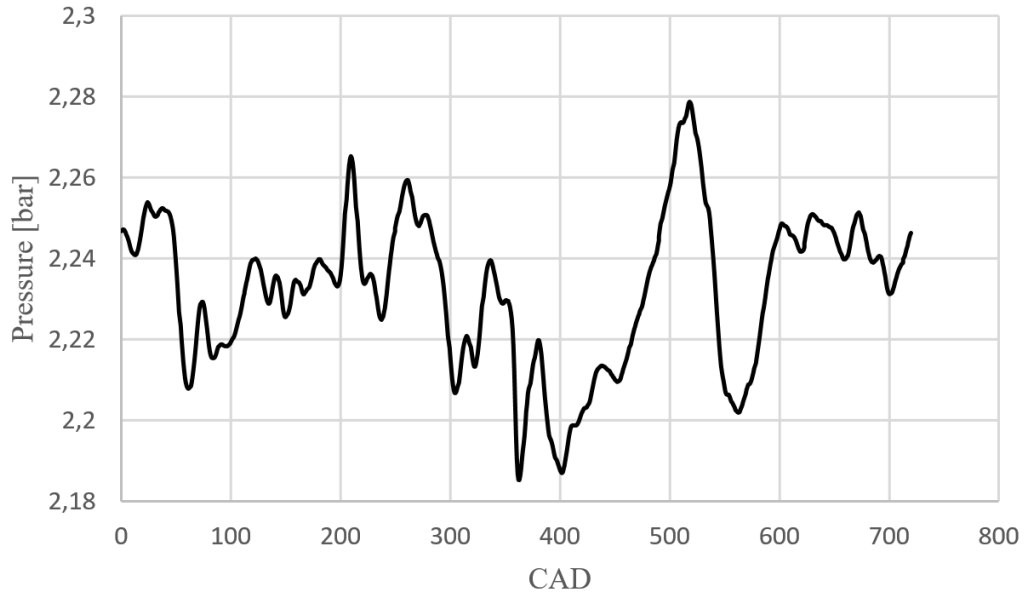


Figure 3.6: Target profile example intake.

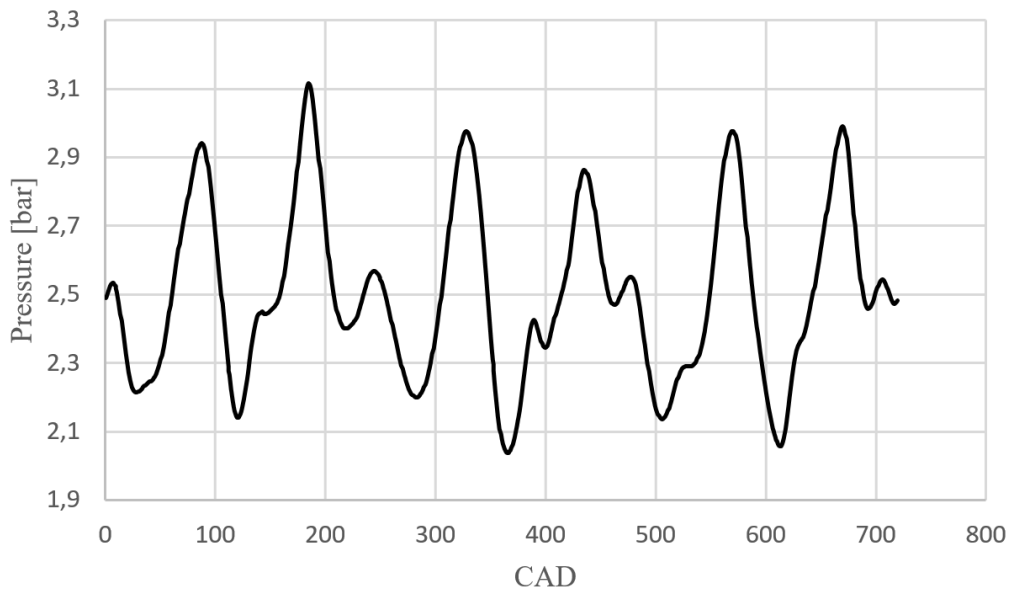


Figure 3.7: Target profile example exhaust.

3.4 Step IV: Changing the combustion volume

As part of the project is dedicated to evaluating the effect of changing the volume of the cylinder, a new cylinder volume is introduced in the model. This is done by replacing the cylinder part of the model with a new cylinder with new cylinder dimensions. As this cylinder is theoretical and no recorded combustion is available a Wiebe combustion model (see Table 2.2) is imposed. Although this limits the flexibility of the model and introduces several simplifications it should not be far from reality. The best geometry modification found in step III is also tried for the changed volume to see the effects of this change. The cylinder dimensions used can be seen in Table 3.2

Table 3.2: Cylinder dimensions.

Case	Volume	Stroke	Bore	Connecting rod length	CR
A	16L	144	165	280	20,13
B	13L	131	158	267,5	20,13

3.5 Model verification

As a last step to validate the model and see whether the model is robust or not, a set of load points outside of the optimization range are tried. These point can be seen in Table 3.3. B1 and B2 are designed to run at as low engine speed as possible for the SCE at the time of the test data collection. One load point is at low load and one at high load. The same goes for B3 and B4. 1400rpm is the max rpm, one low load and one high load point is collected. These load points are at the limit of the operation span of the SCE. The model is not optimised against these load points, they test if the model is valid for a broader operation span or not.

Table 3.3: Verification load points.

Case	Speed	Load	Load/6	EGR%
B1	700	510	85	13,5
B2	700	1740	290	2
B3	1400	306	51	2,5
B4	1400	2832	472	1

4 | Results

In order to give a clear representation of the results, this chapter is structured according to the method section, with gradually increasing complexity. Some guiding comments are given along with the results.

4.1 Step I: Topology and initialization

In step I of the project the main topology of the system was introduced into the simulation software. The dimensions of the system were measured on the actual test rig. These measurements were not perfect but gave an overview of the system. Some simplifications of the inlet were made to reduce the simulation time and the results from these early non-optimized simulation runs can be seen in Figure 4.1, also shown earlier.

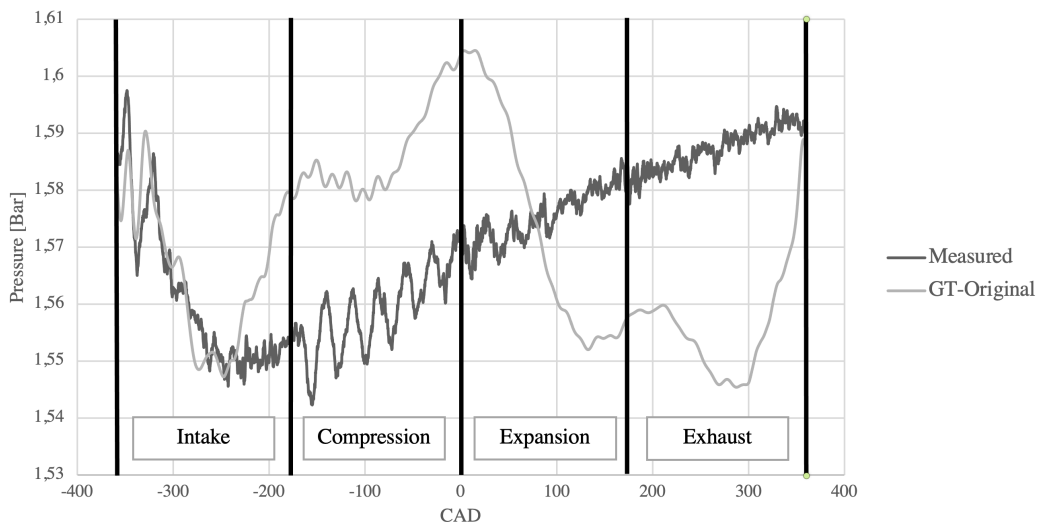


Figure 4.1: Recorded pressure at inlet vs. non-optimized simulated.

The pressure match is far from perfect after this initial step. This case is completely non-optimized and dimensions are in some cases not exact. It can also be seen that the intake valve event pressure closely match (-360CAD - -240CAD), but that the pressure is far off outside this range. The corresponding exhaust pressures can be seen in Appendix A.2

4.2 Step II: Joining models, wave tuning and implementing cylinder pressure

After optimizing the dimensions of the intake and exhaust systems, a better match is found for all tested cases. This is confirmed by the test data. The pressure curve is now followed throughout the whole combustion cycle for both intake and exhaust, as seen in Figure 4.2-4.3 and Appendix A.3-A.8. The dimensions of the intake and exhaust are optimized to mirror the gas dynamics as closely as possible. The figures show that a good match in pressure dynamics has been found for the topology considered, though it must be kept in

mind that these optimizations have been done in a narrow speed range (1000-1200RPM). The result is optimized against a given operation band and might be far off if the whole engine register is considered.

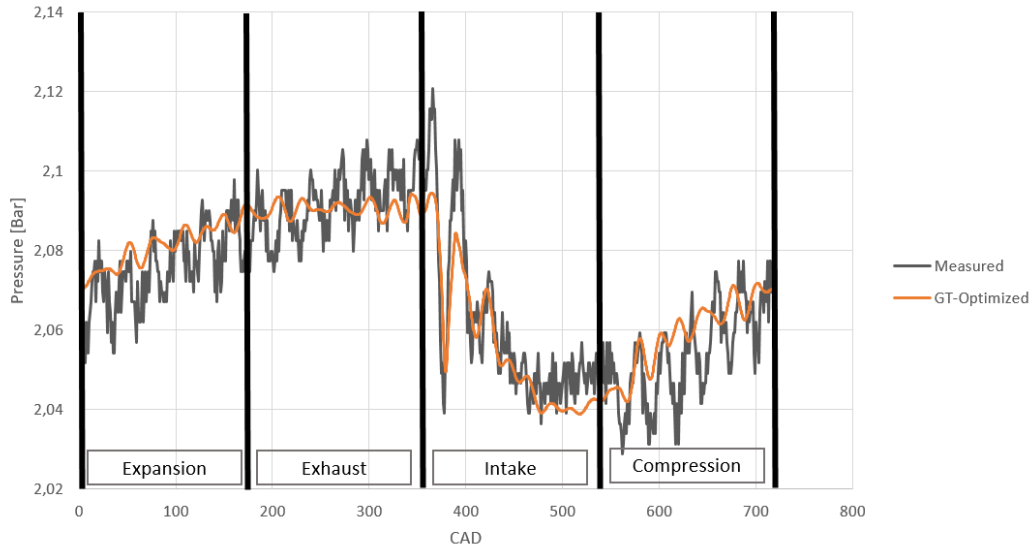


Figure 4.2: Inlet manifold pressure comparison. Measured vs. simulated.

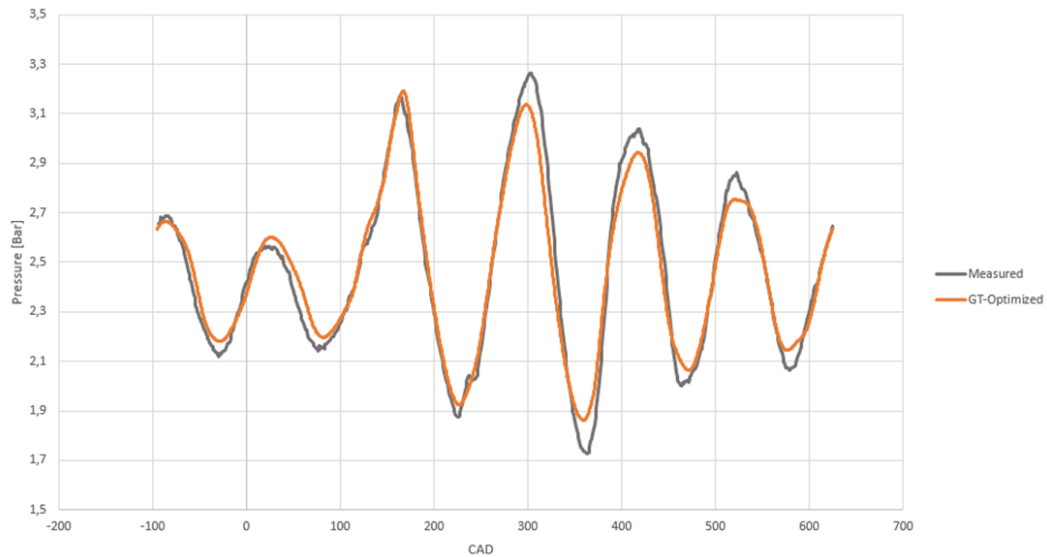


Figure 4.3: Exhaust manifold pressure comparison. Measured vs. simulated.

The implemented combustion model also gave a closer match to the recorded pressure trace from the SCE, as can be seen for one of the cases in Figure 4.4. The simulated pressure follows the measured pressure throughout the whole combustion cycle for both high and low pressure. This shows that the pressure in the cylinder is the same as the

real world case during the valve events meaning the effect of the cylinder in the simulated case should be closely related to the effect of the real world cylinder. The pressure pulses initiated by the cylinder should be more accurate than before and should in turn create more realistic pressure pulses throughout the system. The more accurate combustion also mimics the real combustion temperature better and the temperature of the exhaust pipes should be closer to the real world case.

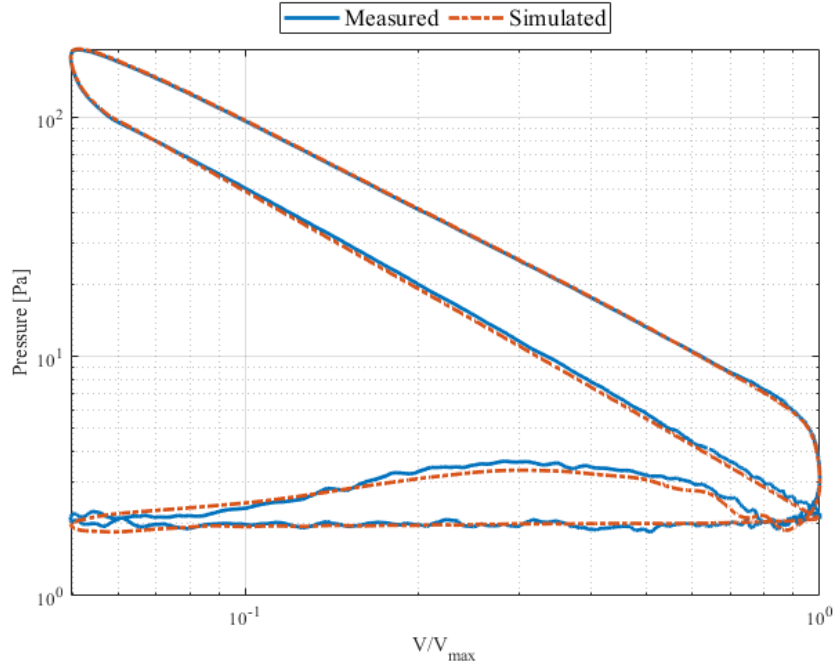


Figure 4.4: Measured vs. simulated pressure trace.

The exhaust back pressure valve on the model is controlled by a PID controller and the general back pressure is set behind the valve. Thus the sensitivity of the system with regards to the back pressure is analyzed, and the results can be seen in Table 4.1 and Figure 4.5. In Table 4.1 the pressure on either side of the back pressure valve can be seen, and in 4.5 the pressure dynamics in the exhaust from the different cases are plotted. Here it can be seen that the pressure behind the exhaust valve has little to no effect on the pressure dynamics upstream of the valve, thus the outlet pressure does not influence the pressure pulses or the combustion. The controller response can be seen in Figure 4.6.

Table 4.1: Exhaust valve pressures on both sides of valve.

Pressure upstream of valve	Pressure downstream of valve
2.4691873	0.90184474
2.4691873	1.0016253
2.4691875	1.1014454
2.4691873	1.2012954
2.4691875	1.3011682

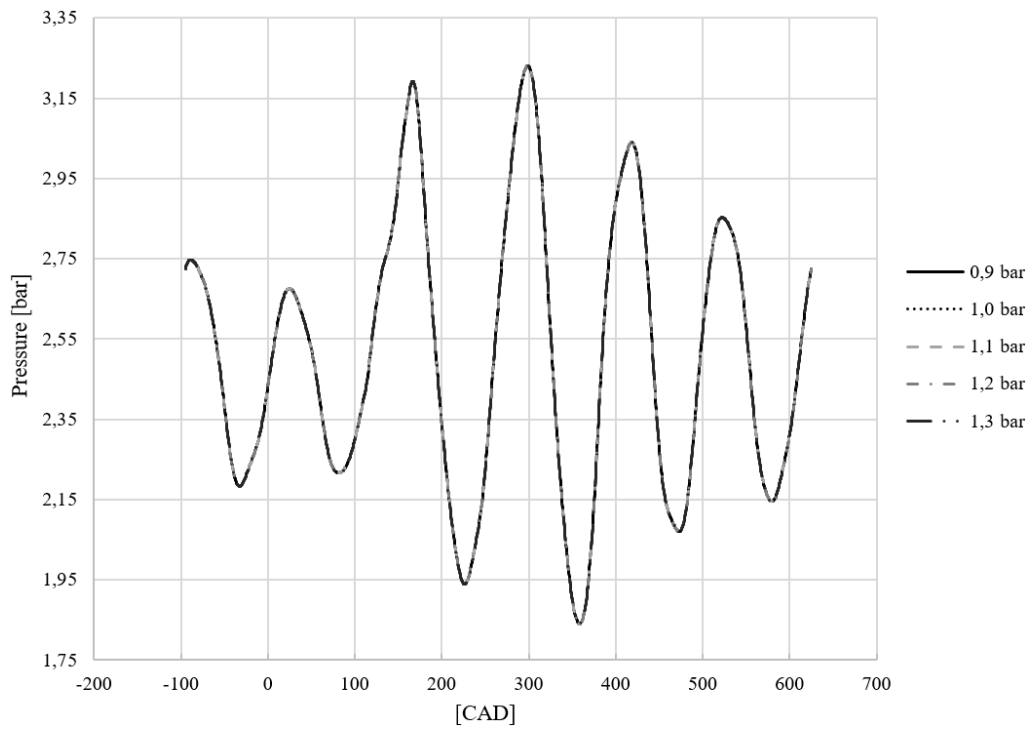


Figure 4.5: Back pressure influence on pressure dynamics.

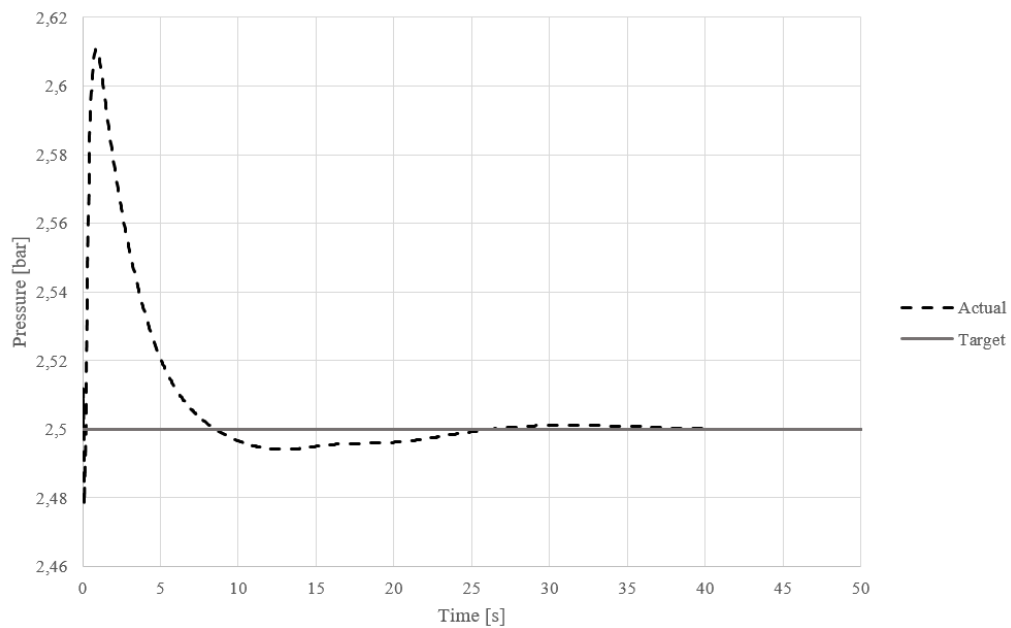


Figure 4.6: Back pressure controller response.

The implementation of the EGR controller showed some system weaknesses (the same behaviour has been seen in the test rig) in regards to controller speed. The EGR-circuit is quite long and the pipes used are of large diameter, which results in a slow EGR-flow. As the exhaust composition is affected by the charge composition and vice versa, the system needs time to stabilize. The controller response can be seen in Figure 4.7.

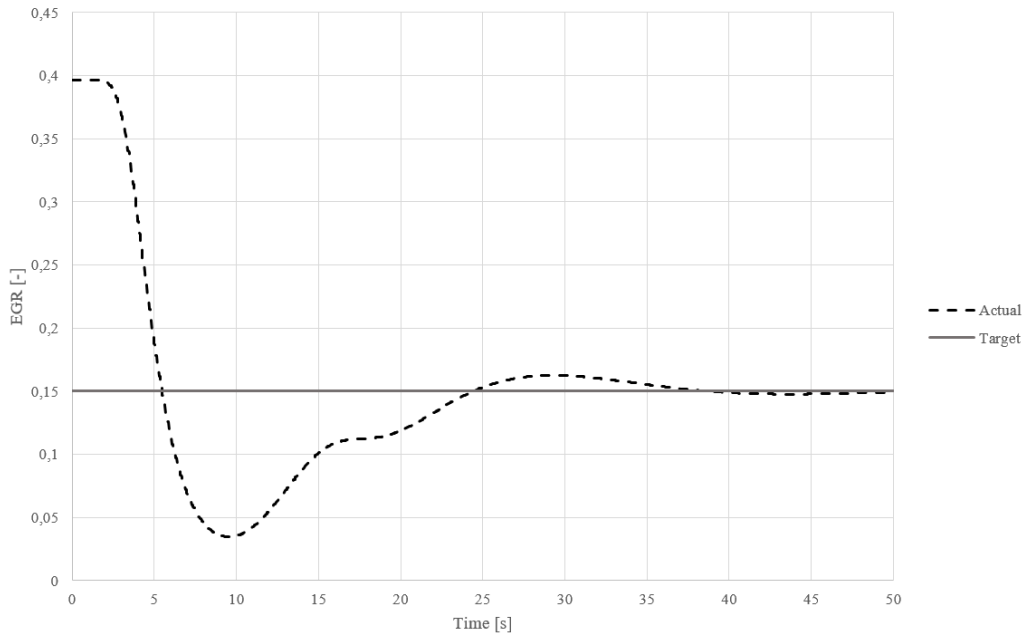


Figure 4.7: EGR controller response.

The back pressure valve and the EGR valve are fighting with each other while controlling the system. This generally requires a slow setting of the control system to not lose stability. In the case of this system the large delay in the EGR is due to the long circuit and its large volume. The model's target value is reached within a time similar to the time for the SCE to reach its target.

4.3 Step III: Topology manipulation and MCE-matching

The implementation of the different concepts seen in Figure 3.5 has different effects on the pressure dynamics as contrasting initial wave dynamics are important. The effect varies with the mean pressure, temperature and flow. Therefore, the effect will be different on the intake side and the exhaust side.

4.3.1 Intake

To apply the various configurations to the intake system, the intake tank is initially replaced with a pipe. The pressure profile imposed by this change is quite different compared to the original in regards to pressure dynamics, and can be seen in Appendix A.15. After this, all the different concepts presented in Figure 3.5 are optimized and each concepts best design is presented in Figure 4.8 below where the target of the optimization is noted as “Measured”. It can be seen that the straight pipe provided a sufficient starting position for each of the concepts to use a large portion of their potential. The closest match is seen in concept A and B with some slight differences. Modifying the topology improves resemblance between measured data and simulated data, even though the amplitudes are

not captured correctly. The setup closely matches the initial pressure drop during early valve opening and somewhat mirrors the returning pressure wave during the middle of the intake opening. It is a large improvement compared to the present installation in the rig, which here is noted as “Original”.

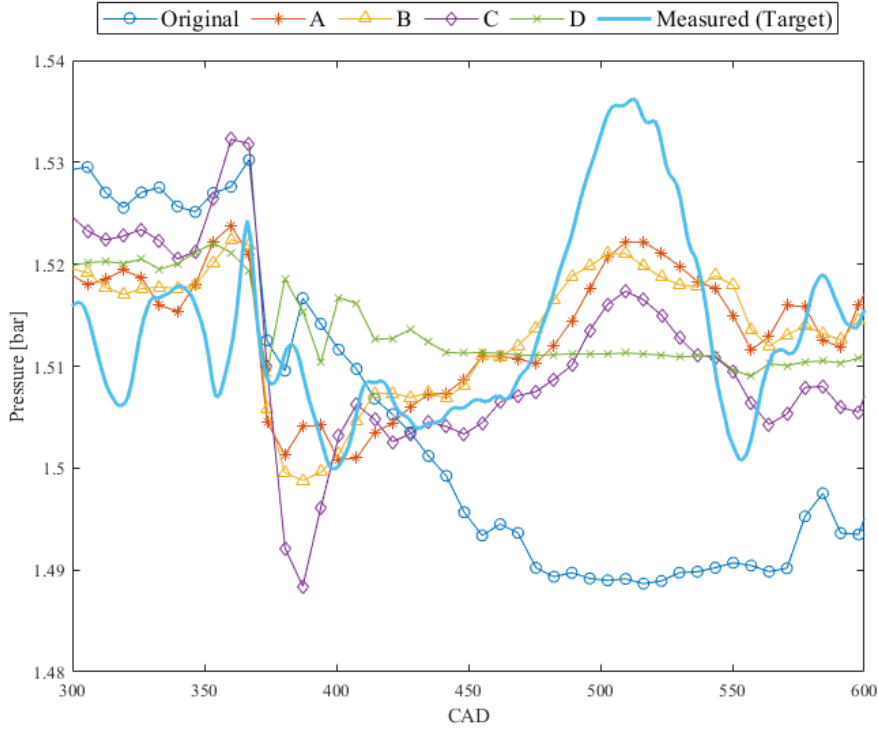


Figure 4.8: Intake configuration effect on pressure dynamics. Original is the current installation, A-D are the modifications and Measured (Target) is the 6-cylinder target profile.

4.3.2 Exhaust

Compared to the intake, the exhaust pulses are harder to modify. This is due to the larger pressure fluctuations, both in the MCE and the SCE. Both the magnitude and phasing of the pressure peaks and valleys need to be modified. This makes the exhaust an overall more complex operation. In figure 4.9 the pulses for the different concepts can be seen. The presented curves are for the optimized geometry for each design. Three more figures for other load points can be seen in Appendix A.19-A.21. There are three main pressure peaks and three main valleys visible during the time the exhaust valve is open. It can be seen that all concepts manage to match the amplitude of the first pressure peak in the MCE closer than the original configuration. The second smaller peak is however only captured by concept A and C. The third peak is captured relatively well by all concepts except for D. A similar resemblance of the valley is achieved by all designs. Concept D is however further off than the others in the second valley but slightly closer than the others in the last valley. This is due to the different phase. The phase is off at the last valley even though the amplitude is closer. The match differs slightly depending on load point but holds true in general.

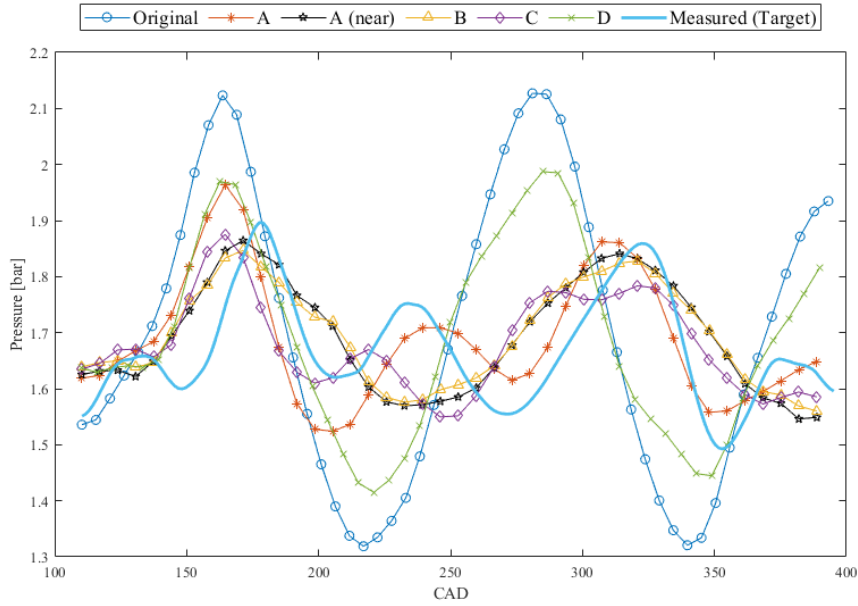


Figure 4.9: Exhaust configuration effect on pressure dynamics. Original is the current installation, A-D are the modifications and Measured (Target) is the 6-cylinder target profile.

When considering the best modification of intake side of the system, the A modification seem to give the best result. The geometry allowances were limited at a diameter and length that seemed large but the optimizer quickly found the optimization limit to be the best option. Therefore it is assumed that a very large offshoot is beneficial to the pressure pulses. Modification A and modification B both performed well but due to a lower complexity A is deemed the preferable design. In Figure 4.10 the proposed final design schematic can be seen. In Table 4.2 the dimensions of the flow modifications can be seen and in Figure 4.11 the winning designs notations can be found.

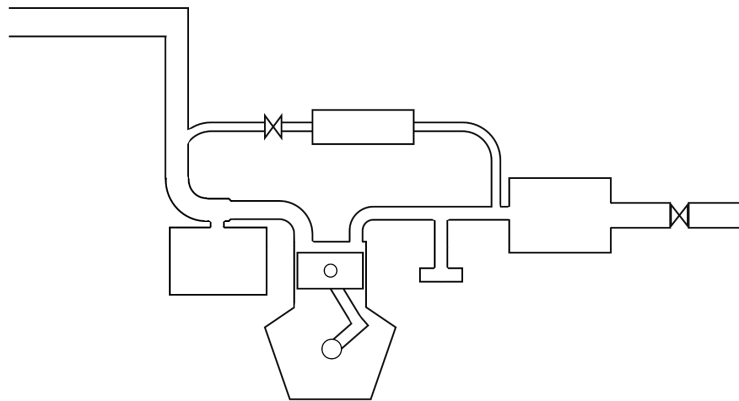


Figure 4.10: Schematic of the final optimized design. Note the added volumes on the exhaust and intake side.

The best match of the MCE pressure trace in the SCE considering the exhaust side was also concept A. A long pipe with a disc shaped volume at the end, mounted a bit further away from the exhaust port. This design manages to catch the second pressure peak as mentioned in section 4.3.2, which only concept A and C did. Concept A had an overall better match when all load points were considered, and is therefore considered the best design.

Table 4.2: Dimensions of best design concepts.

Dimension*	Intake [mm]	Exhaust[mm]
Inner Diameter	70	49
Inner Length	10**	418
Outer Diameter	1000***	277
Outer Length	1041	82

* Notation description found in Figure 4.11

** Minimum of optimization bound. *** Maximum of optimization bound.

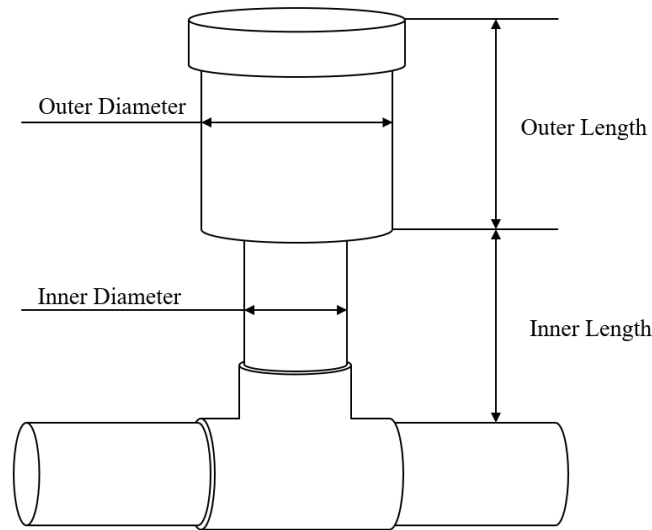


Figure 4.11: Notation description.

4.4 Step IV: Changing the combustion volume

The effect of changing the combustion chamber volume is shown in Figure 4.12- 4.13 and Appendix A.11-A.12, where the comparison between 16L and 13L can be seen in regards to pressure in intake and exhaust.

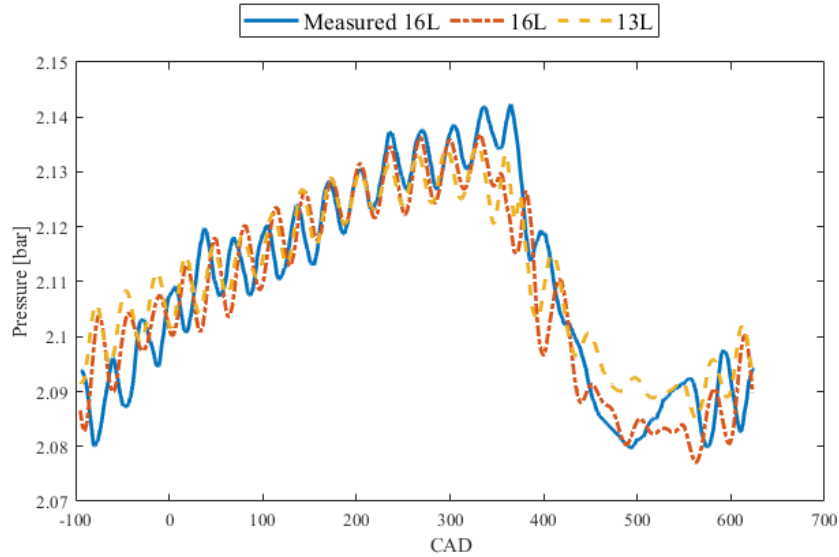


Figure 4.12: Comparison of intake side pressure dynamics for variation of displaced volume of engine. Measured (16L) and simulated values (13 and 16L).

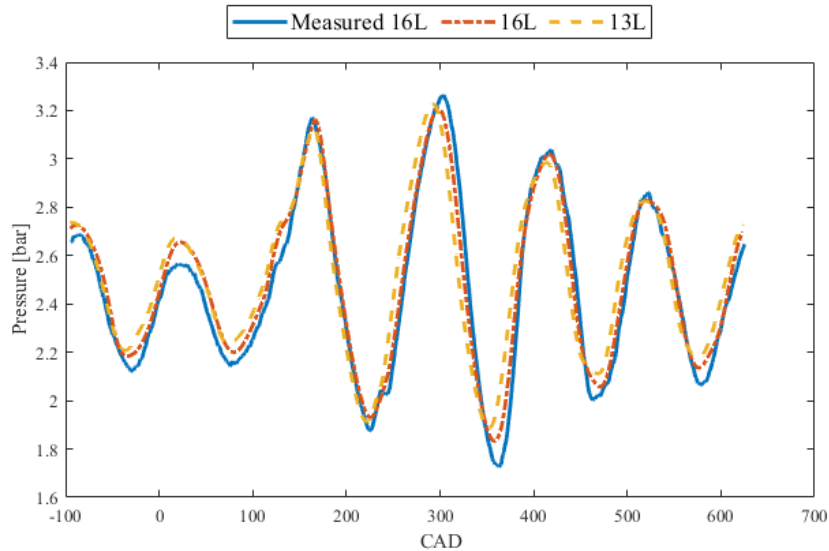


Figure 4.13: Comparison of exhaust side pressure dynamics for variation of displaced volume of engine. Measured (16L) and simulated values (13 and 16L).

Given the original intake and exhaust topology the change in pressure dynamics due to cylinder volume is quite small. The most obvious difference can be seen in Figure 4.12

where the pressure drop does not reach the same level during the end of induction (450-550CAD). In Figure 4.13, apart from the slight mismatch in phasing, the exhaust pressures match quite well. The effect of changing the topology to the one optimized for the 16L while using a 13L cylinder can be seen in Figure 4.14 and 4.15.

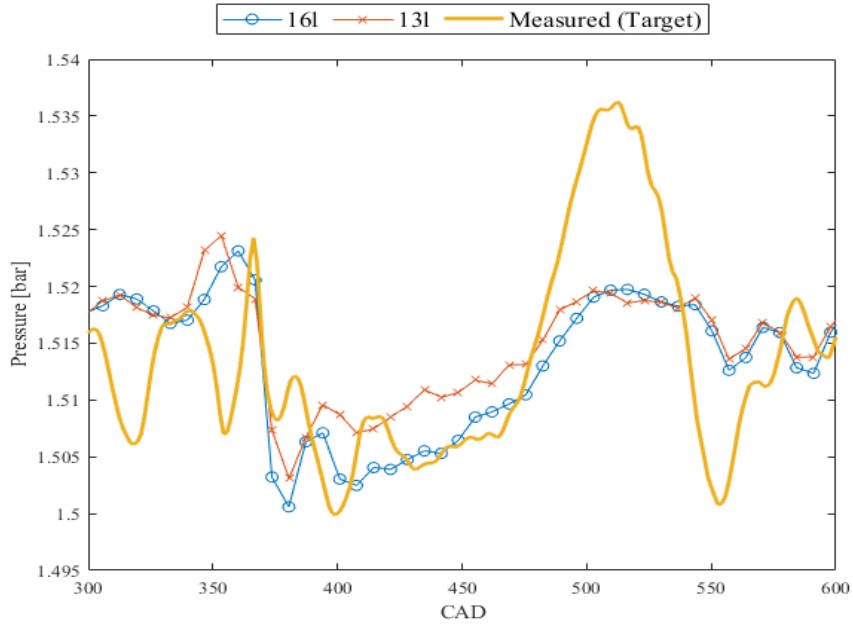


Figure 4.14: Comparison of intake pressure dynamics with modification. Simulated 16L and 13L 1-cyl, and simulated 16L 6-cyl.

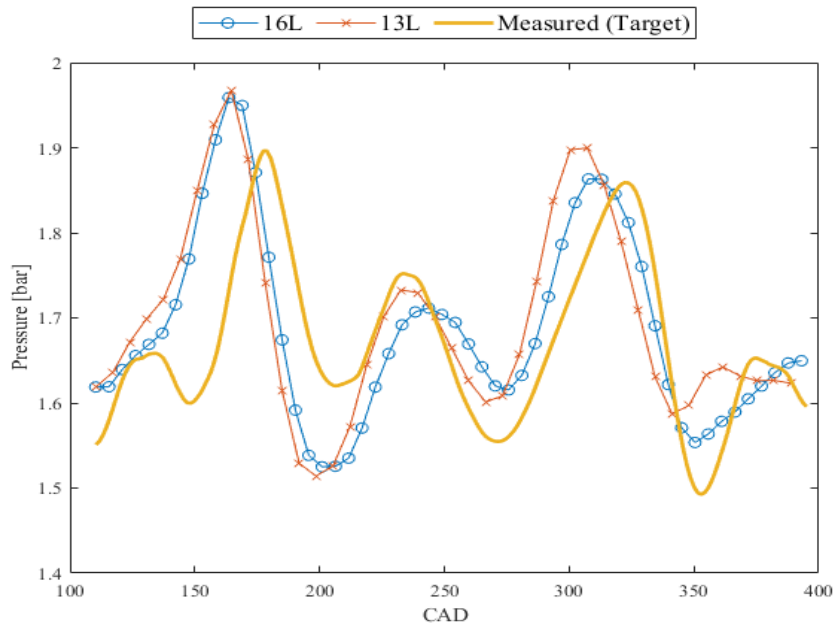


Figure 4.15: Comparison of exhaust pressure dynamics with modification. Simulated 16L and 13L 1-cyl, and simulated 16L 6-cyl.

4.5 Model verification over broader range

To verify the model a further set of load points are run in the SCE, seen in table 3.3. The same points are then tested in the model. The comparison of simulated vs. measured data for all extended load cases can be seen in Figures 4.16-4.19 and A.22-A.25.

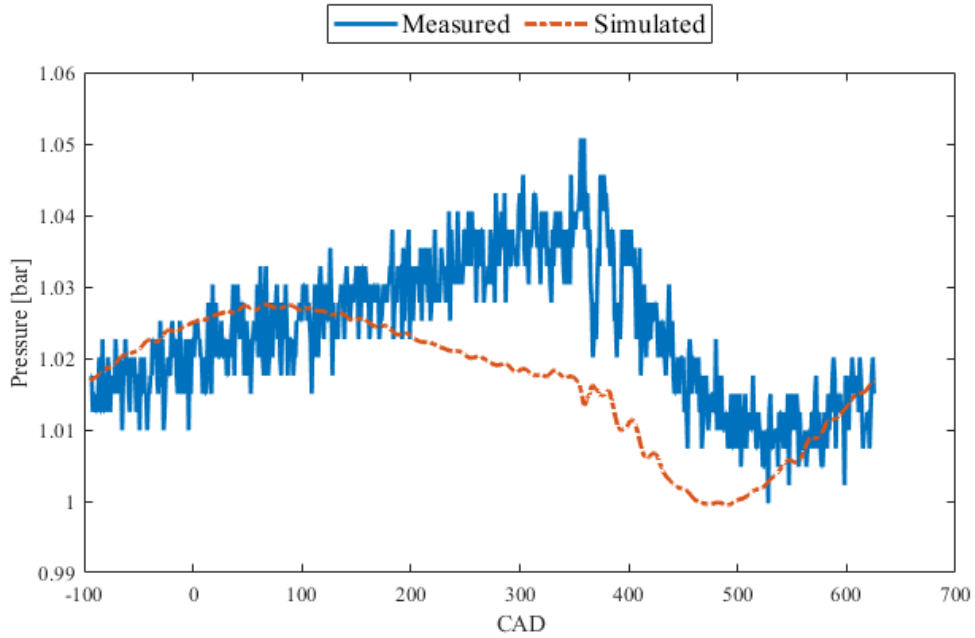


Figure 4.16: Comparison of pressure dynamic responses, in the intake. 700rpm 85Nm.

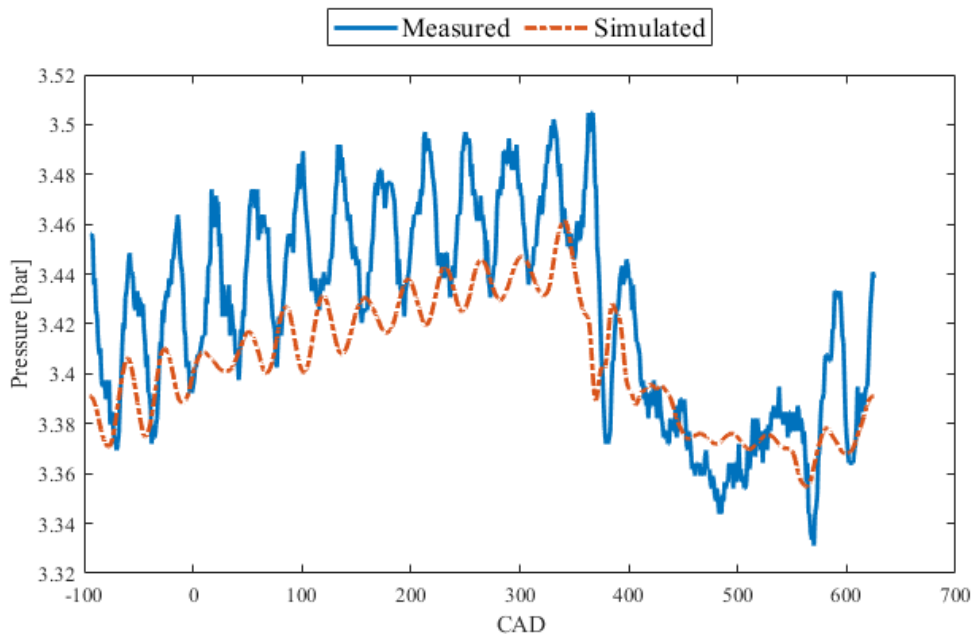


Figure 4.17: Comparison of pressure dynamic responses, in the intake. 1400rpm 472Nm.

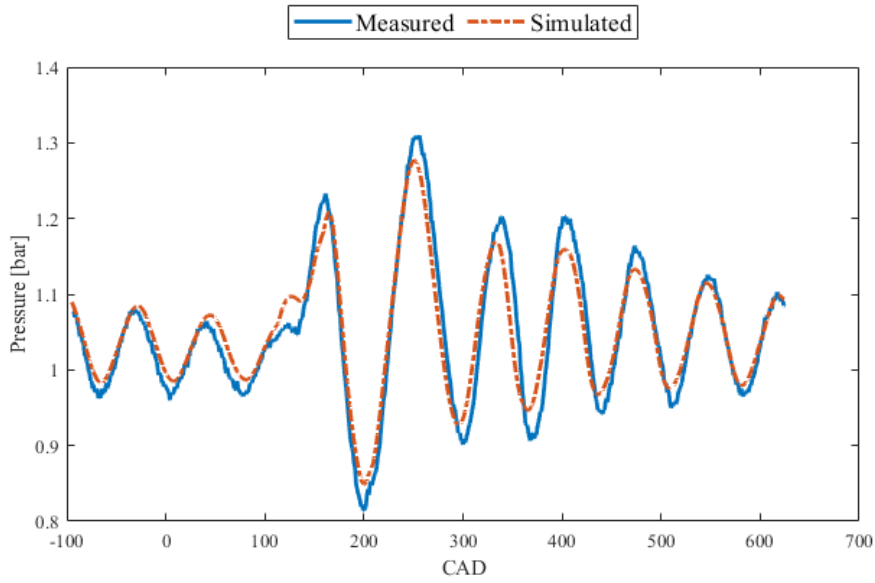


Figure 4.18: Comparison of pressure dynamic responses, in the exhaust. 700rpm 85Nm.

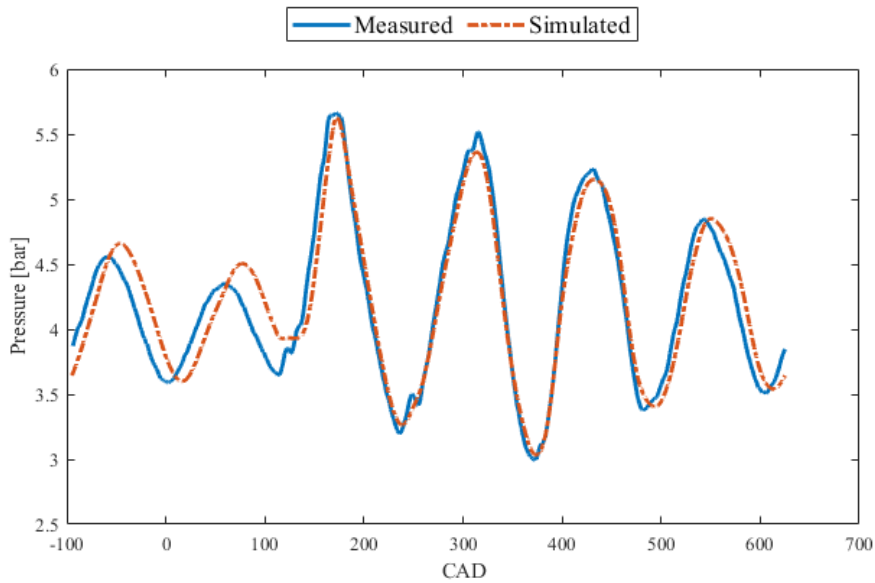


Figure 4.19: Comparison of pressure dynamic responses, in the exhaust. 1400rpm 472Nm.

The validation run shows a good correlation between the pressure dynamics, especially in the exhaust. The amplitudes and overall shape are close between experimental and simulated curves. In the intake however, the low speed cases are off in regards to the shape of the pressure traces. In the high speed cases the shape follows closer but show an overall lower pressure. As seen in the figures the pressure amplitudes are still close in regards to the pressures, around 0,03 bar.

5 | Discussion

From the results presented it can be seen that the added geometries can provide the SCE with a better pressure correlation to that of the MCE in both intake and exhaust. The intake system currently installed on the single-cylinder research engine is difficult to optimize in a fair way in 1D, and due to the complex unsteady flow throughout the fluid circuit a 3D GT-model approach is unfavourable due to time and convergence stability. This results in a simplified geometry (seen in Figure 3.3) which is optimized to mimic the pressure dynamics of the SCE, whereas the optimal method firstly would mimic the geometry which in turn would recreate the pressure dynamics. This method is thus sensitive to operating conditions for which the geometry is not optimized for as the geometry might only provide satisfactory results for the initial points considered.

Figure 4.16 shows that the simulated intake pressure trace for 700rpm have a slightly different pressure dynamics and characteristics than the measured. The scale on the y-axis should however be noted. The difference in peak pressure is in the magnitude of 0,02 bar. This means that even though the pressure trace looks different the pressure is in a close region. The same goes for the high load 700rpm case seen in Appendix A.22. This means that the intake side of the model does not resemble the real world SCE at low speeds, but this mostly applies to the shape of the curve. This is most likely attributed to the transformation from 3D reality to 1D modelling and the use of a small set of load points for optimization. To achieve a better match throughout the engine range a better intake model must be made. Due to the nature of the intake tank a 3D model might be appropriate and more load points would be beneficial.

The 1400rpm are on the other hand different. The pressure trace for the high load can be seen in figure 4.17, and the low load in appendix A.23. The shape of the pressure curves are now a closer match. The model is deemed appropriate for simulating medium and high speeds.

The pressure traces for the exhaust side are seen in figure 4.18-4.19 and appendix A.24-A.25. The pressure is followed in a good manor for all cases. The pressure peaks and valleys are of similar magnitudes and the phases are close. The exhaust side of the model is a good replication of the physical SCE for all cases tried and is thus deemed valid for all operating conditions.

As the number of possible modifications to the geometry of the system are endless, only a small portion are considered. The geometries considered will thus be the only ones selected and implemented. It is possible and likely that several other modifications would result in better pressure correlations, but the tried modifications showed that better solutions exist and further work might unveil modifications that prove themselves even better.

The implementation of the 13L cylinder showed a small difference in the intake. The induction does not lower the pressure as much as the 16L does. This is intuitive as the smaller cylinder accepts a smaller volume of gas and therefore the pressure will not decrease as much. On the exhaust side the pressures are extremely close, both in amplitude and

phasing. The general effect of changing to a 13L cylinder can thus be deemed small and no major differences arise. When the 13L engine is installed with modifications the pressure dynamics are still comparable to the 16L engine with modification and no big difference can be seen.

An issue that arose when implementing the EGR controller was the slow rate at which the EGR travels through the EGR circuit. The EGR circuit is in the SCE relatively long at more than 4 meters and a total volume of about 20 liters when disregarding the distance from cylinder to EGR inlet and outlet. This is much larger than in any MCE. It should also be kept in mind that the SCE only uses one cylinder and the flow rates will thus be much lower and will result in even slower EGR flow rates compared to the MCE. Also, if the cylinder would be smaller (13L) this problem would be even more apparent. To get around this problem the EGR circuit length and volume should be minimized as much as possible without creating a severe flow restriction compared to the EGR valve to maintain the possibility of utilizing a high EGR flow.

6 | Conclusion

There are significant differences in the gas exchange between the single- and 6-cylinder engines, mainly the pressure dynamics in the intake and exhaust. The average pressure are close to identical, but the dynamics are different and out of phase to each other.

A GT-Suite model for the for a 16L equivalent engine is successfully created and verified for all simulated load points. The model is shown to be a close representation of the physical engine, in both the intake and the exhaust pressure dynamics, as well as the in cylinder pressure.

The GT-suite model is modified to represent the 6-cylinder pressure dynamics during the valve event as this is where the fluid flow in and out of the cylinder takes place. This is done using modifications to the intake and exhaust. The modifications that captured the pressure dynamics best in the intake is to first remove the existing intake tank and replace it with a pipe. Then a large tank is added to the side of the intake pipe, with dimensions according to figure 4.11 and table 4.2. The modification that captured the pressure dynamics best in the exhaust is to add a pipe with a hollow disc on its end, perpendicular to the exhaust pipe, which dimensions can be seen in figure 4.11 and table 4.2. These modifications improved the pressure dynamics and captures the pulses in a closer way when compared o the original setup in both intake and exhaust.

The displacement volume change, going from a 16L equivalent to a 13L equivalent, shows no significant impact in regards to pressure dynamics. With the added modifications previously mentioned, the result is similar. There are no significant change in the shape of the pressure dynamics curve, and the same goes for the magnitude.

7 | Future work

To continue and improve the model a series of recommendations are made. The model is optimized towards data that is acquired from a MCE engine model and not from an actual MCE engine. Measuring fast pressure traces in the intake and exhaust of an engine would verify the data and give more insight into the pressure pulses present.

Moreover, a DI-Pulse combustion model (see Table 2.2) should be set up for the engine. This model would allow the model to run at different load points without specific setup. Using the TPA model (see Table 2.2) or the DI Wiebe model limits the combustion to predetermined combustion profiles as the models are imposed combustion models. As of now the model is verified within a small operating window and needs specific setup for each case.

Furthermore the model would be improved if more load points would be used for optimization. The DI-Pulse model requires many operating points, which also could be used for optimization purposes.

Additionally, adding more geometry modifications to the intake and exhaust system could result in a better optimization and a better pressure pulse match.

Bibliography

- [1] “World oil outlook 2020,” Organization of the Petroleum Exporting Countries, 2020, www.opec.org.
- [2] “Policy brief 16, interlinkages between energy and transport,” United Nations, 2018.
- [3] “Global transportation energy and climate roadmap,” The International Council on Clean Transportation, 2012, www.theicct.org.
- [4] “Färdplan för fossilfri konkurrenskraft: Fordonsindustrin - tunga fordon,” Fossilfritt Sverige, 2020. [Online]. Available: https://fossilfritt.sverige.se/wp-content/uploads/2020/09/Fardplan__Tunga-fordon.pdf
- [5] G. Kalghatgi, “Development of fuel/engine systems—the way forward to sustainable transport,” *Engineering*, vol. 5, no. 3, pp. 510–518, 2019. [Online]. Available: <https://www.sciencedirect.com/science/article/pii/S2095809918305940>
- [6] J. B. Heywood, *Internal Combustion Engine Fundamentals*. New York, USA: McGraw-Hill, 1988.
- [7] H. Heisler, *Vehicle and engine technology, 2nd edition*. Oxford, Great Britain: Elsevier, 1999.
- [8] W. A. Majewski and H. Jääskeläinen, “Engine emission control,” February 2021. [Online]. Available: https://dieselnet-com.eu1.proxy.openathens.net/tech/engine__emission-control.php
- [9] P. Punov and T. Evtimov, “Combustion optimization in a modern diesel engine by means of pre-injection strategy,” in *trans & MOTAUTO '15*, 2015.
- [10] M. K. Khair and H. Jääskeläinen, “Diesel fuel injection,” February 2021. [Online]. Available: https://dieselnet-com.eu1.proxy.openathens.net/tech/diesel__fi.php
- [11] —, “Combustion in diesel engines,” February 2021. [Online]. Available: https://dieselnet-com.eu1.proxy.openathens.net/tech/diesel__combustion.php
- [12] —, “Exhaust gas recirculation,” November 2020. [Online]. Available: https://dieselnet-com.eu1.proxy.openathens.net/tech/engine__egr.php
- [13] H. Z. N. Ladommatos, S. Abdelhalim, “Control of oxides of nitrogen from diesel engines using diluents while minimising the impact on particulate pollutants,” *Applied Thermal Engineering*, vol. 18, no. 11, pp. 963–980, 1998. [Online]. Available: <https://www.sciencedirect.com/science/article/pii/S1359431198000313>
- [14] *GT-SUITE, Engine Performance Application Manual*, Gamma Technologies, Westmont, USA, 2021.
- [15] *GT-SUITE, Flow Theory Manual*, Gamma Technologies, Westmont, USA, 2021.
- [16] *GT-SUITE, Optimization Manual*, Gamma Technologies, Westmont, USA, 2021.
- [17] E. J. Heller, *Why You Hear What You Hear*. Princeton, USA: Princeton University, 2012.

A | Appended figures

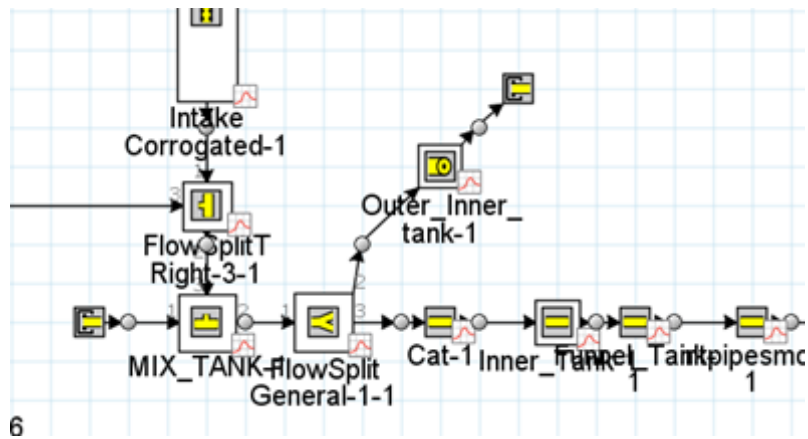


Figure A.1: GT-Power modelled tank.

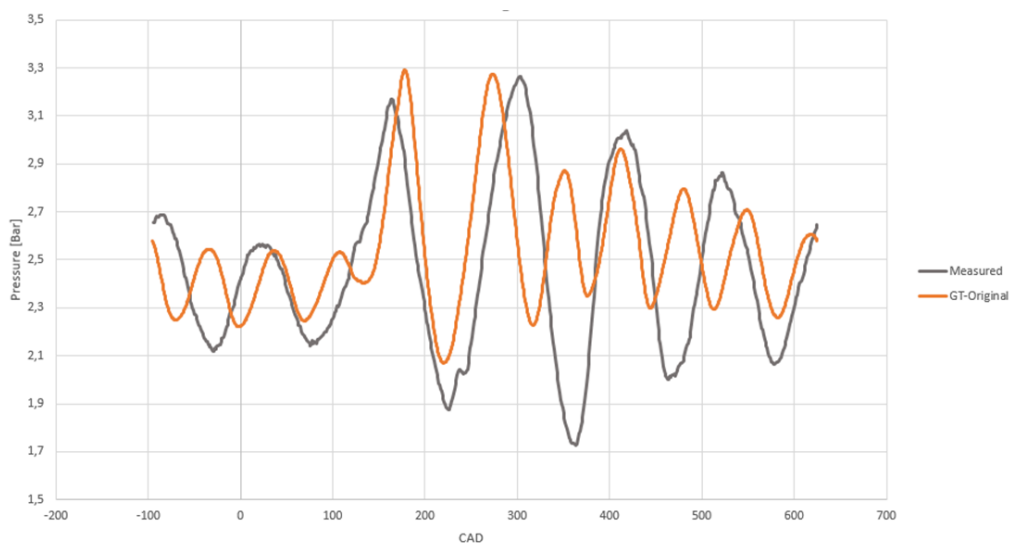


Figure A.2: Recorded pressure at exhaust vs. non-optimized simulated.

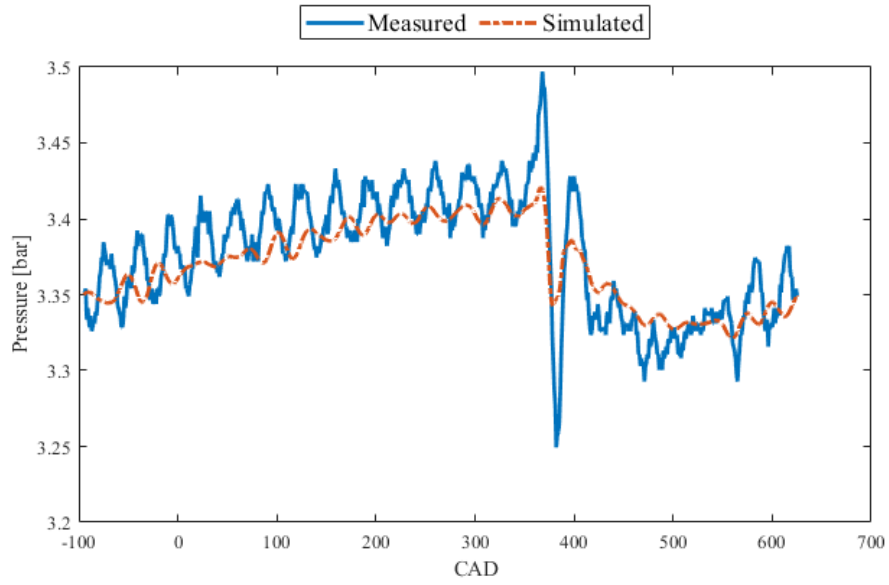


Figure A.3: Comparison of pressure dynamic responses based on volume, in the intake. Case 1.

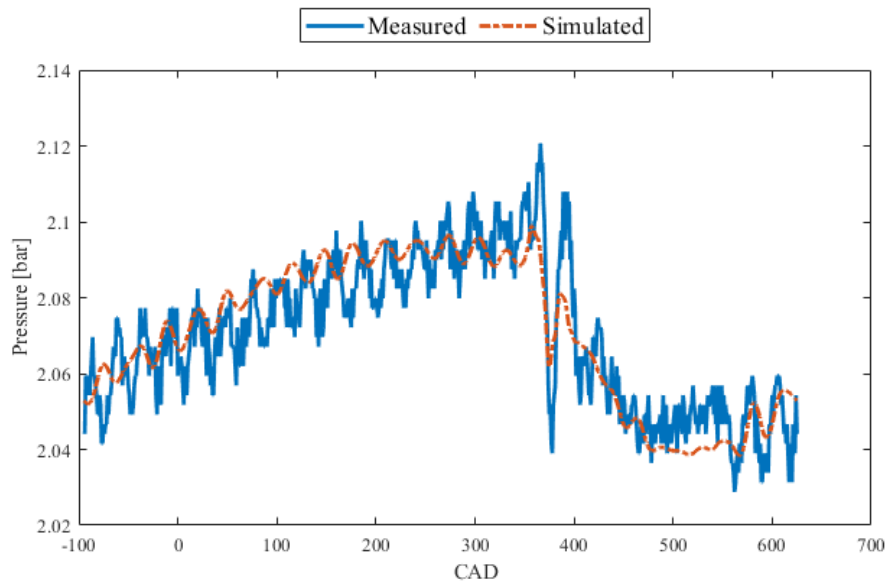


Figure A.4: Comparison of pressure dynamic responses based on volume, in the intake. Case 3.

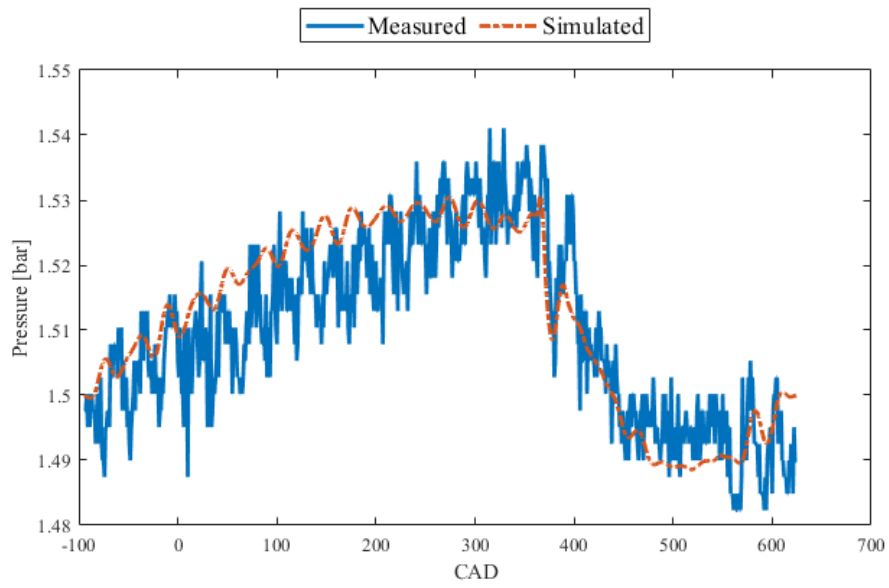


Figure A.5: Comparison of pressure dynamic responses based on volume, in the intake. Case 4.

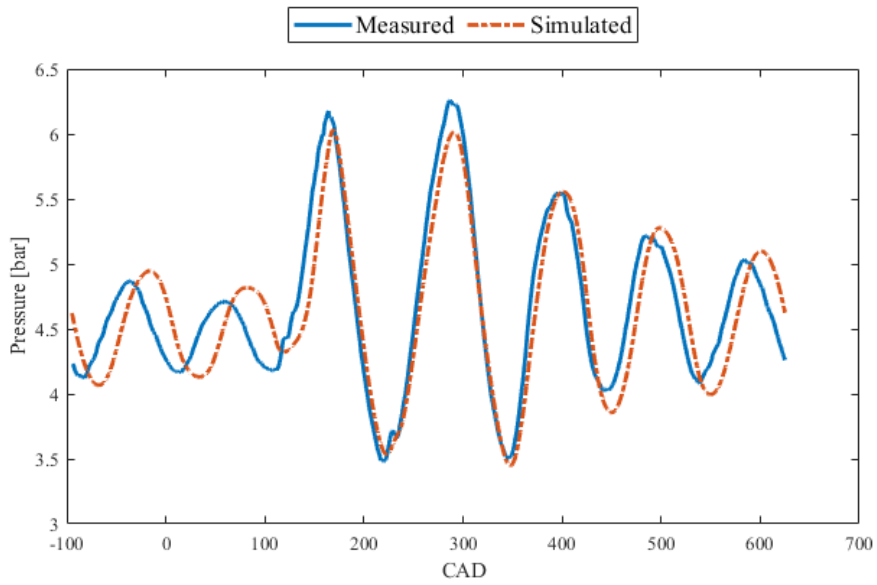


Figure A.6: Comparison of pressure dynamic responses based on volume, in the exhaust. Case 1.

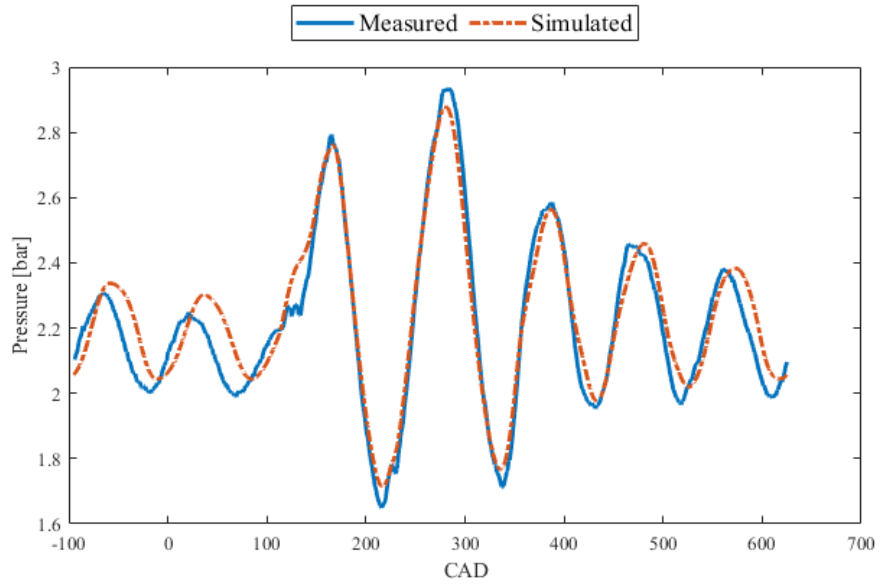


Figure A.7: Comparison of pressure dynamic responses based on volume, in the exhaust. Case 3.

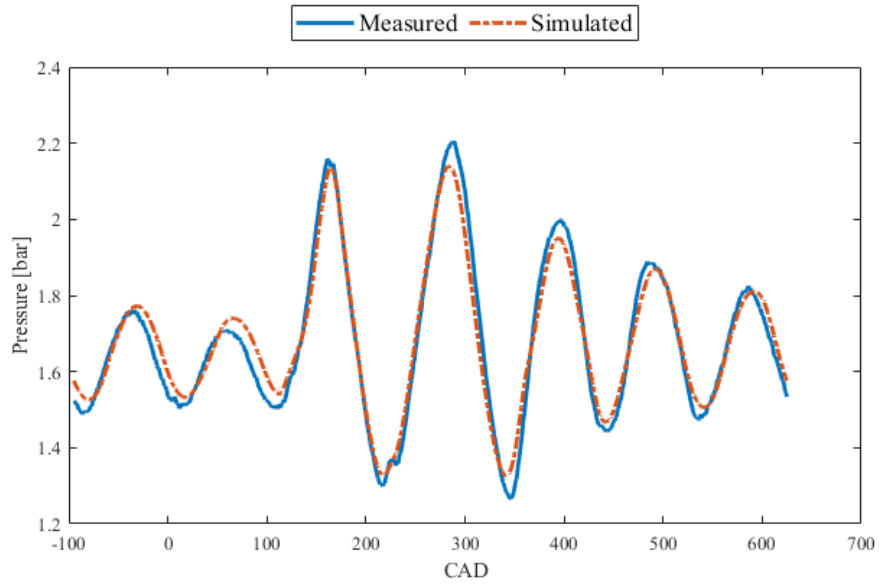


Figure A.8: Comparison of pressure dynamic responses based on volume, in the exhaust. Case 4.

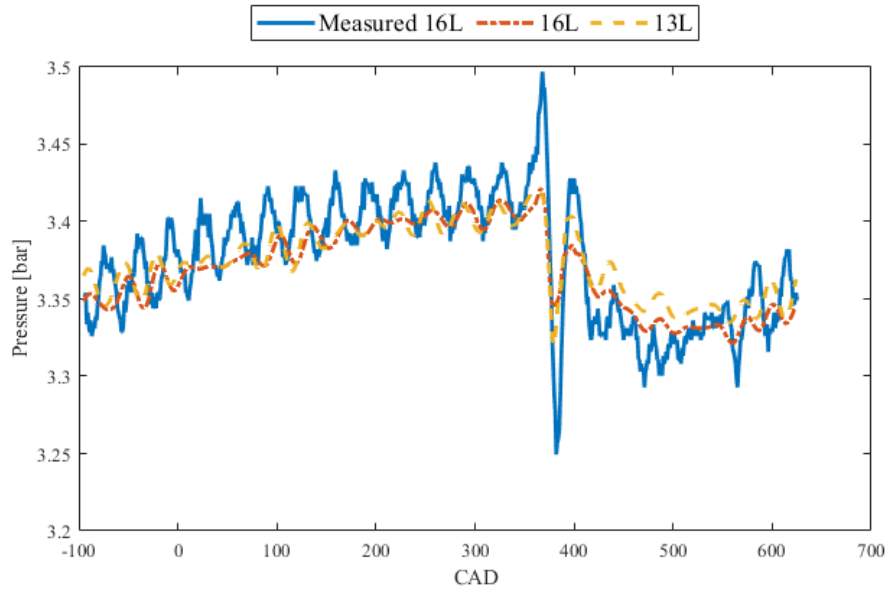


Figure A.9: Comparison of pressure dynamic responses based on volume, in the intake. Case 1.

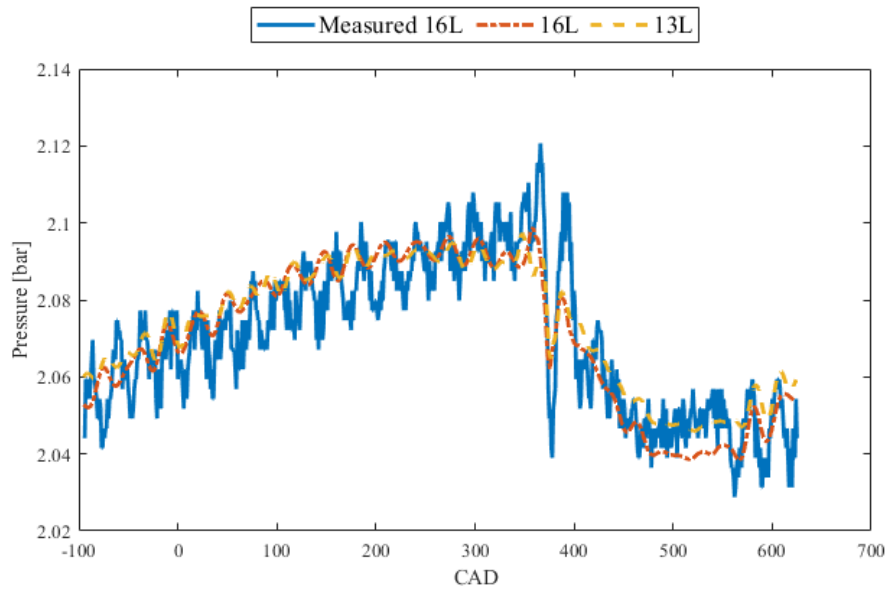


Figure A.10: Comparison of pressure dynamic responses based on volume, in the intake. Case 3.

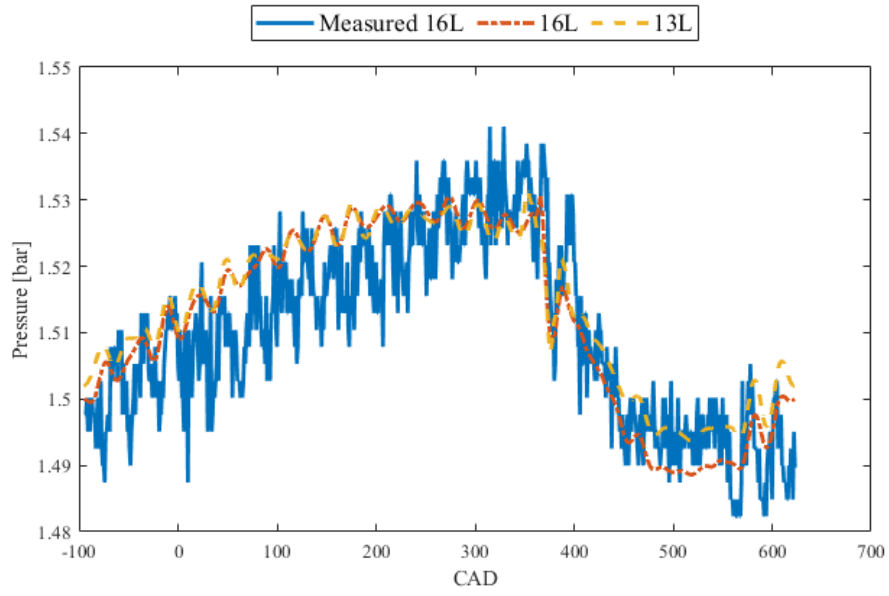


Figure A.11: Comparison of pressure dynamic responses based on volume, in the intake. Case 4.

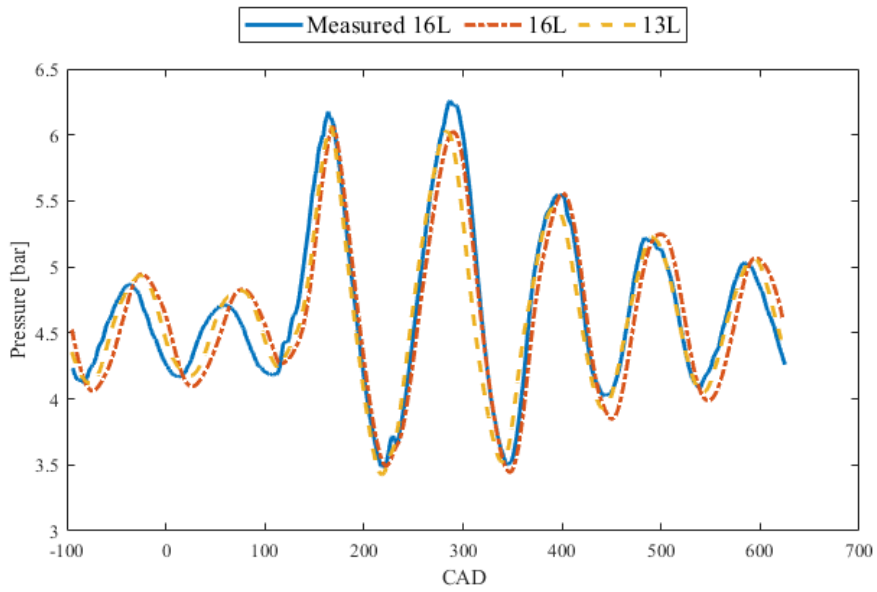


Figure A.12: Comparison of pressure dynamic responses based on volume, in the exhaust. Case 1.

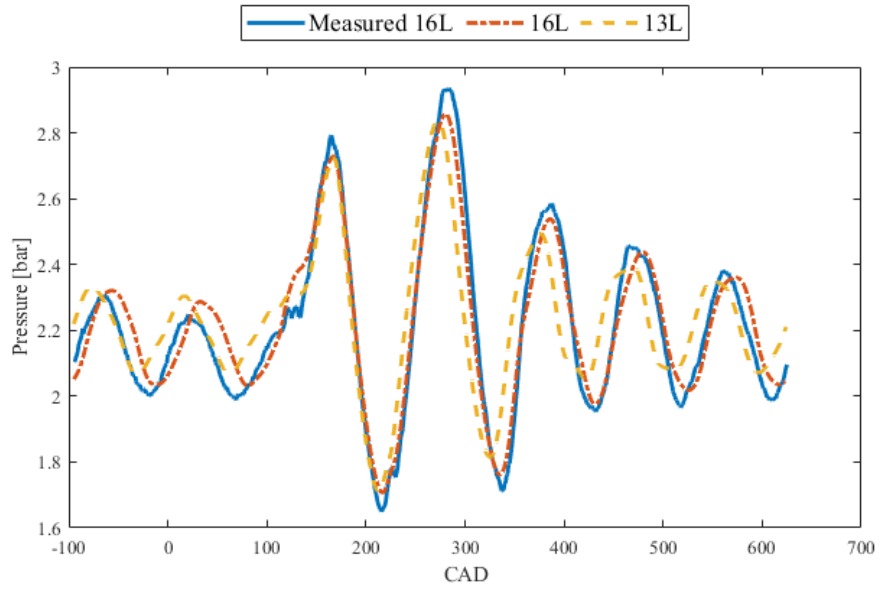


Figure A.13: Comparison of pressure dynamic responses based on volume, in the exhaust. Case 3.

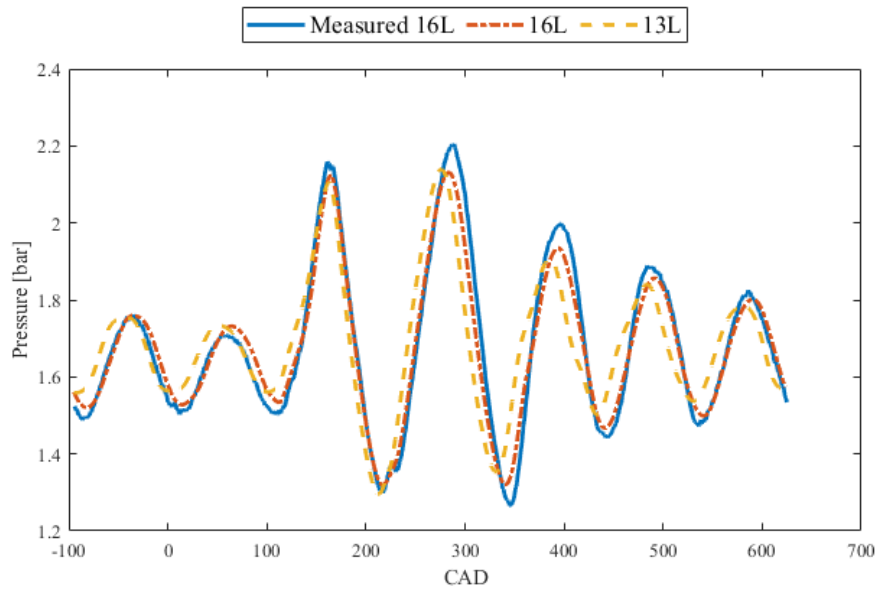


Figure A.14: Comparison of pressure dynamic responses based on volume, in the exhaust. Case 4.

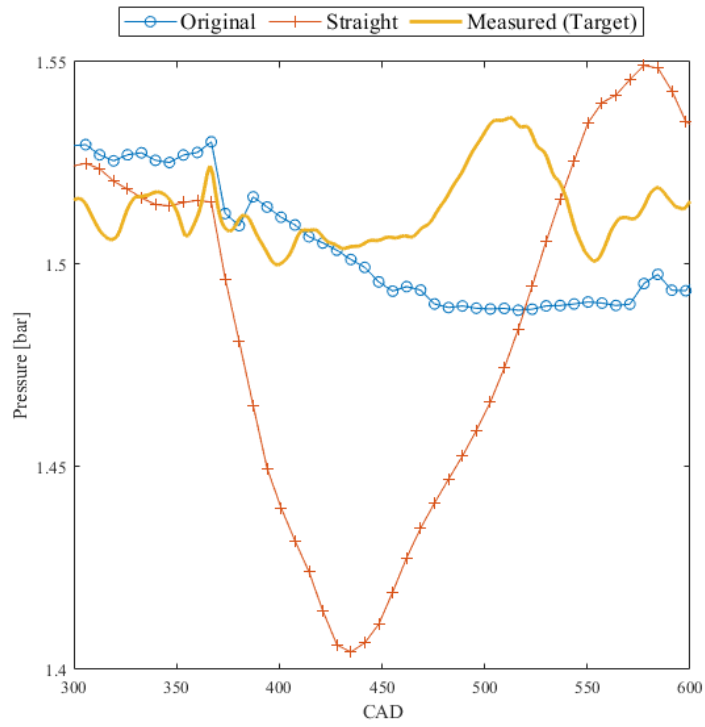


Figure A.15: Comparison of original, straight pipe without modifications and target pressure dynamics.

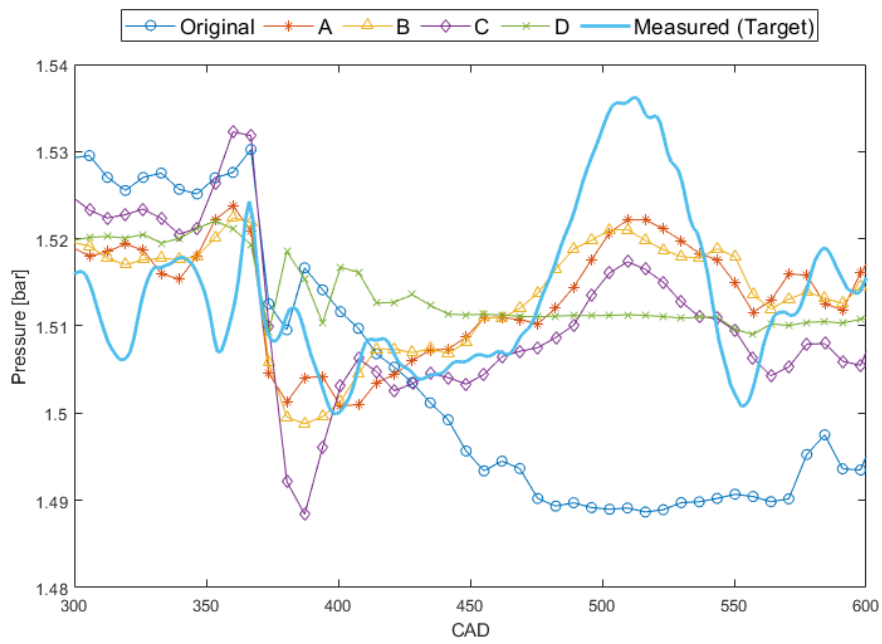


Figure A.16: Comparison of pressure dynamic responses in intake from suggested configurations. Case 1.

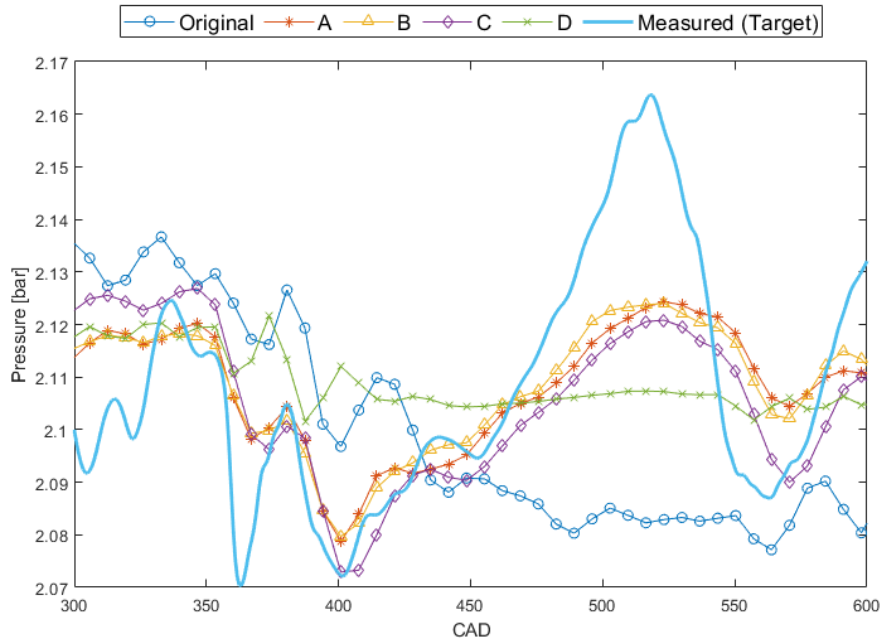


Figure A.17: Comparison of pressure dynamic responses in intake from suggested configurations. Case 2.

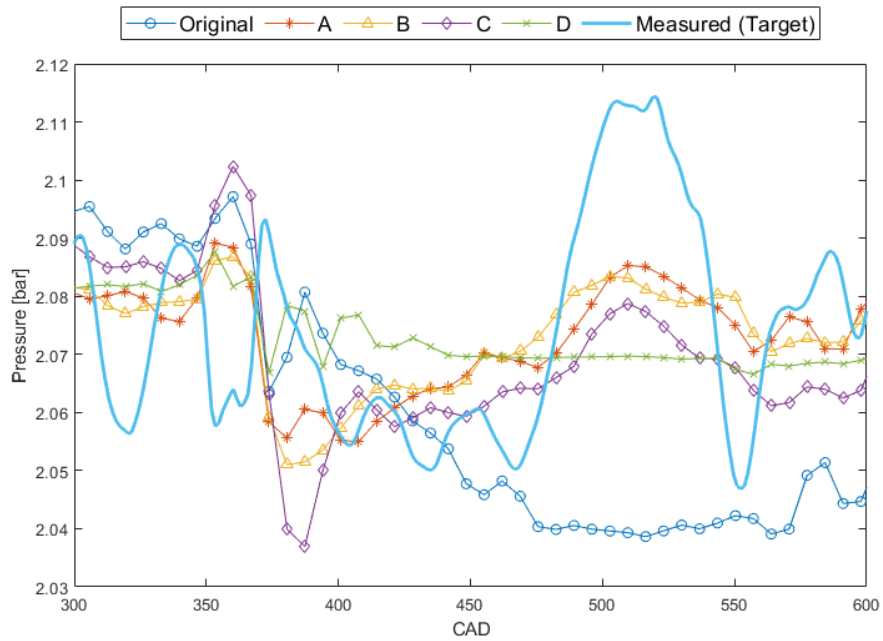


Figure A.18: Comparison of pressure dynamic responses in intake from suggested configurations. Case 3.

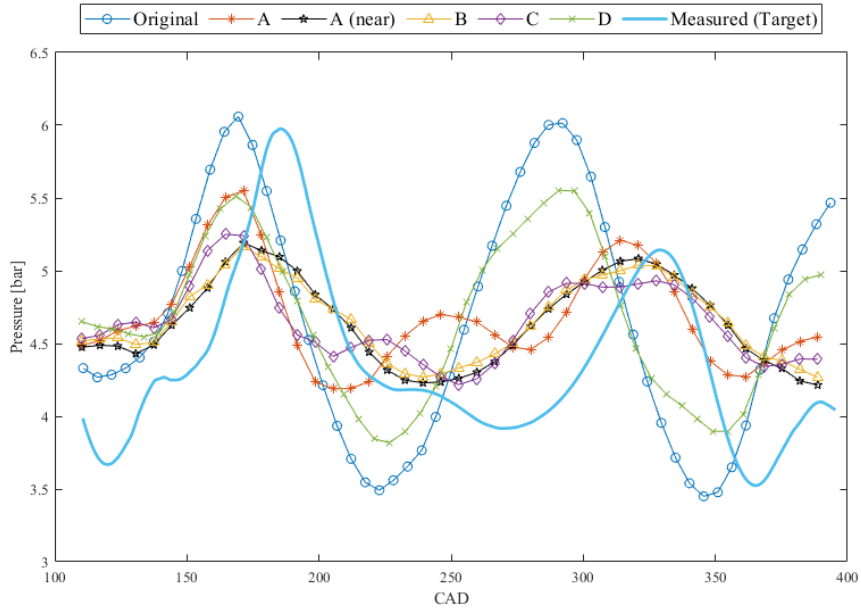


Figure A.19: Comparison of pressure dynamic responses from suggested configurations. Case 1.

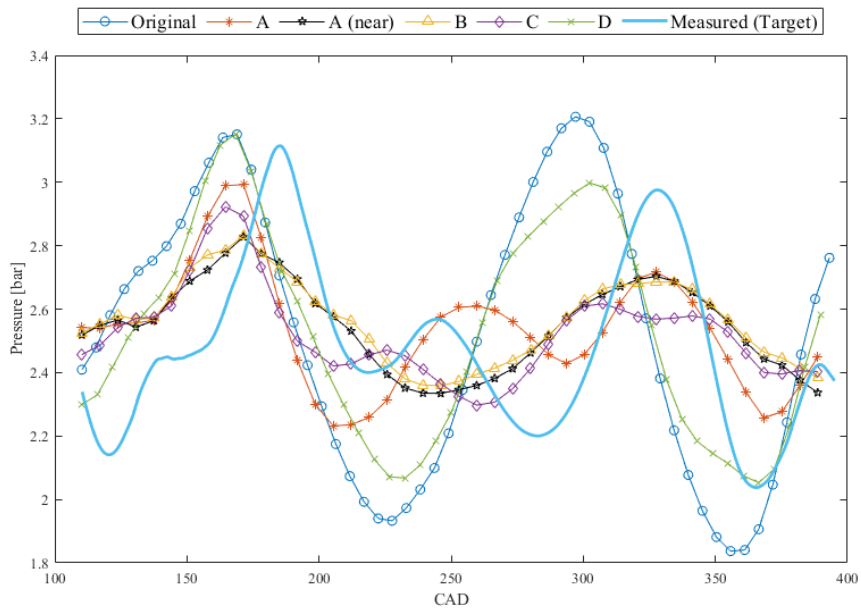


Figure A.20: Comparison of pressure dynamic responses from suggested configurations. Case 2.

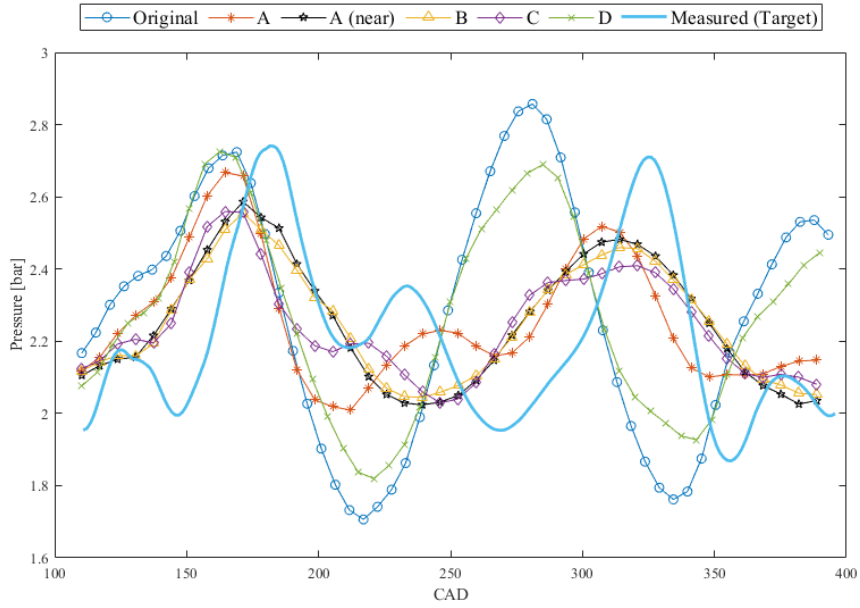


Figure A.21: Comparison of pressure dynamic responses from suggested configurations. Case 3.

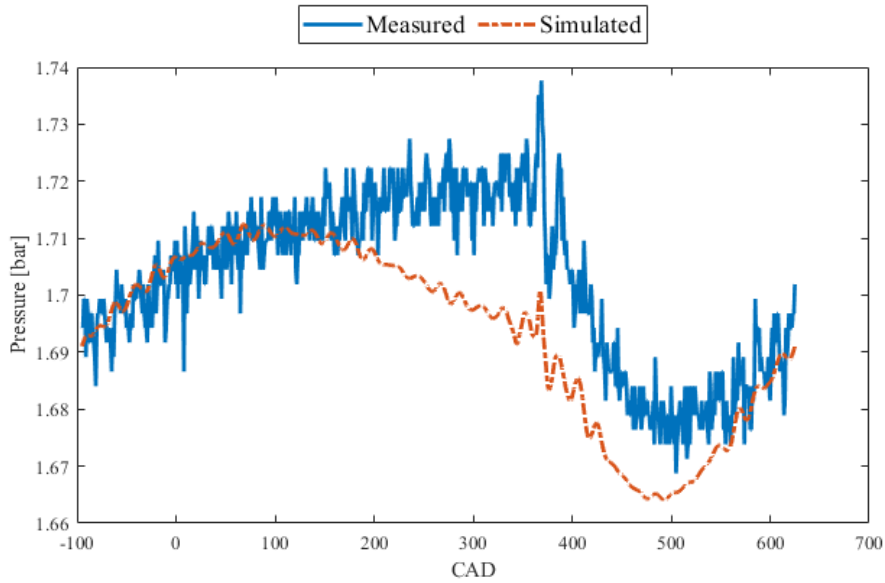


Figure A.22: Comparison of pressure dynamic responses, in the intake. 700rpm 290Nm.

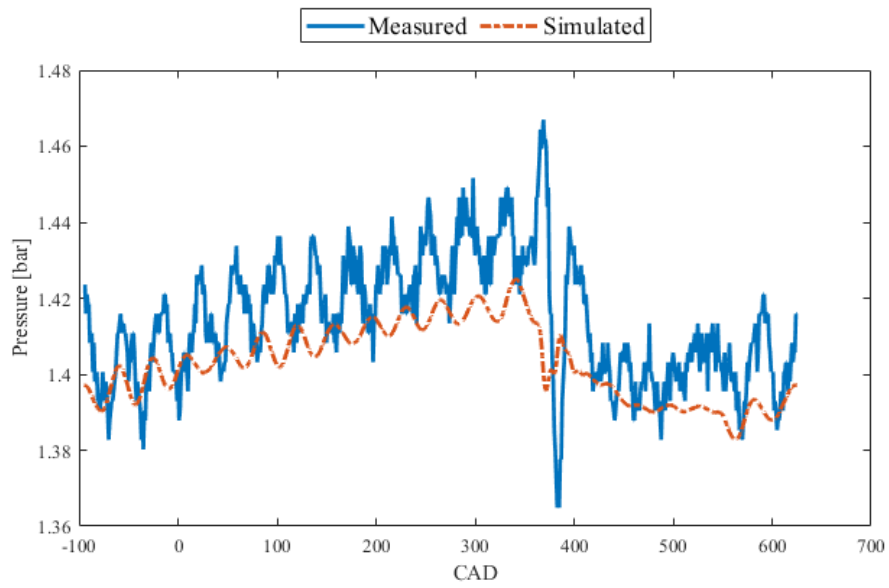


Figure A.23: Comparison of pressure dynamic responses, in the intake. 1400rpm 51Nm.

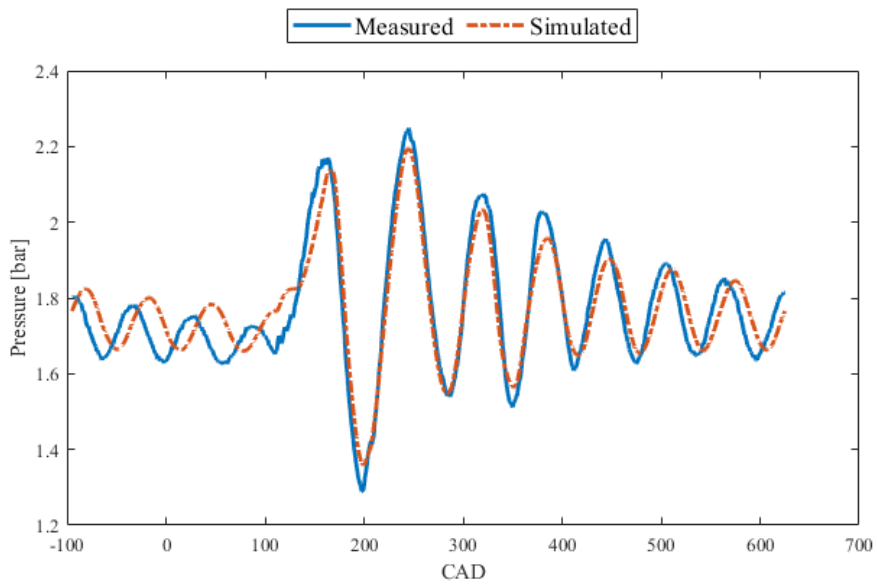


Figure A.24: Comparison of pressure dynamic responses, in the exhaust. 700rpm 290Nm.

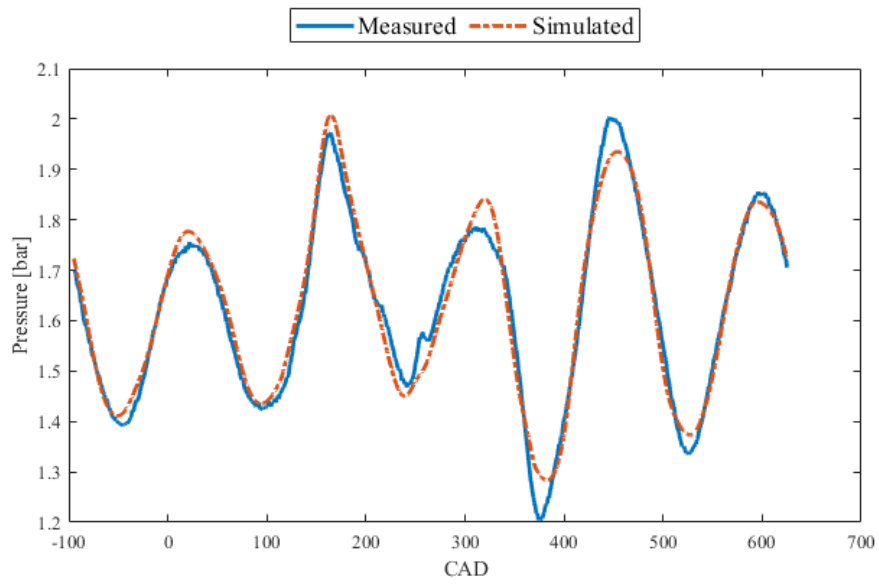


Figure A.25: Comparison of pressure dynamic responses, in the exhaust. 1400rpm 51Nm.

DEPARTMENT OF MECHANICS AND MARITIME SCIENCES
DIVISION OF COMBUSTION AND PROPULSION SYSTEMS
CHALMERS UNIVERSITY OF TECHNOLOGY

Gothenburg, Sweden
www.chalmers.se



CHALMERS
UNIVERSITY OF TECHNOLOGY